UNCLASSIFIED

AD 274 170

Reproduced
by the

ARMED SERVICES TECHNICAL INFORMATION AGENCY
ARLINGTON HALL STATION
ARLINGTON 12, VIRGINIA
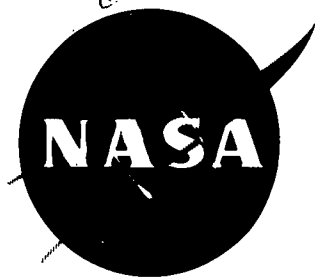
UNCLASSIFIED

NASA

TECHNICAL NOTE

D-1197

EXPERIMENTAL STUDY OF THE EFFECTS OF WEIGHTLESSNESS

ON THE CONFIGURATION OF MERCURY AND

ALCOHOL IN SPHERICAL TANKS

By Donald A. Petrash, Robert F. Zappa,
and Edward W. Otto

Lewis Research Center
Cleveland, Ohio

NATIONAL AERONAUTICS AND SPACE ADMINISTRATION

WASHINGTON   April 1962

NATIONAL AERONAUTICS AND SPACE ADMINISTRATION

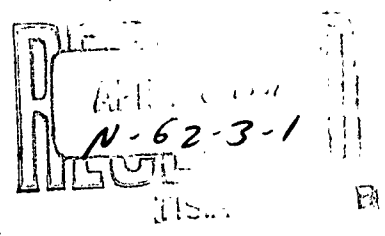
TECHNICAL NOTE D-1197

EXPERIMENTAL STUDY OF THE EFFECTS OF WEIGHTLESSNESS

ON THE CONFIGURATION OF MERCURY AND

ALCOHOL IN SPHERICAL TANKS

By Donald A. Petrash, Robert F. Zappa,
and Edward W. Otto

SUMMARY

As a part of the overall study of the problems associated with the behavior of rocket engine propellants stored in space-vehicle tanks while exposed to weightlessness and solar and planetary radiant heat sources, the zero-gravity liquid configuration of several common liquids in spherical glass tanks was experimentally investigated.

The zero-gravity equilibrium liquid configuration for mercury in spherical glass tanks is one in which the liquid-vapor surface is a surface of constant curvature and the mercury remains in contact with the walls at the same contact angle as was observed in the 1-g environment. The contact angle for mercury appeared to be unaffected by the level of the gravity field.

The zero-gravity equilibrium liquid configuration for ethyl alcohol in spherical glass tanks is a completely wetted tank wall with a spherical vapor bubble in the interior of the liquid.

The time required to wet the tank wall completely increased with an increase in the ratio of density to surface tension for carbon tetrachloride, ethyl alcohol, and water.

INTRODUCTION

The NASA Lewis Research Center is currently conducting a study of the problems associated with the behavior of rocket-engine propellants stored in space-vehicle tanks while exposed to weightlessness and solar and planetary radiant heat sources. The condition of weightlessness will be encountered by space vehicles during planetary oribital missions and during periods of coast on interplanetary space missions. A knowledge of the final equilibrium liquid configuration will be needed to

solve the problems of effective tank venting, pump inlet design, orientation control of space vehicles, and effective long-term propellant storage. The mechanics of heat transfer to stored propellants during periods of weightlessness must be determined because the bouyant forces that normally remove vapor bubbles from tank walls are absent, as are convective-heat-transfer processes. As a part of this overall study, the liquid-configuration dynamics of several common liquids are being experimentally investigated in a weightless environment without heat input.

In general, the forces acting on a liquid are the inertial forces and the intermolecular forces that are exhibited in the form of the surface-tension forces. When a liquid is under the influence of a gravity field, the inertial forces predominate, and only small effects of the surface-tension forces are noticeable. Typically, the effects of dominant inertial forces are the shaping of liquids in tanks, the weight of the liquid, the hydrostatic pressure of liquid columns, the rise of vapor bubbles in liquids due to bouyancy, and the convection currents in liquids as a result of heat inputs. The effects of the surface-tension forces are exhibited by the meniscus of liquids in contact with solid bodies and by the capillary rise or depression in small-diameter tubes.

However, when a liquid is removed from the effects of a gravity field, the surface-tension forces become significant because the inertial forces are no longer dominant. Hence, the equilibrium liquid configuration, the liquid-configuration dynamics, and the mechanics of heat transfer are influenced to a larger degree by the surface-tension forces.

These problem areas are currently under study, both analytically and experimentally, by several investigators in the field of weightlessness. Analytical studies of the behavior of liquids, both wetting and nonwetting, in the absence of gravitational forces were undertaken by Li (ref. 1) and Benedikt (refs. 2 to 4). Experimental studies of the behavior of liquids, both wetting and nonwetting, in the absence of gravity forces have been conducted by Reynolds (ref. 5), Usiskin and Siegel (ref. 6), Siegel (ref. 7), Brazinsky and Weiss (ref. 8), Steinle (ref. 9), Neiner (ref. 10), and Sherley (ref. 11).

The purpose of this report is to present and discuss the experimental results obtained from an investigation of the equilibrium liquid configuration of typical wetting and nonwetting liquids in spherical glass tanks in a weightless environment in the absence of heat inputs. These results were obtained over a range of tank sizes and fillings. A 1.95-second period of weightlessness was obtained in a drop tower in which the experimental package was subjected to a free fall. The test procedures utilized ensured extremely quiescent initial conditions and a gravity level below 10^{-5} g. It should be noted that hereinafter the terms weightlessness and zero gravity will be used synonymously.

DISCUSSION OF ANALYTICAL CONCEPTS

The history of the study of surface-tension phenomena can be traced as far back as Leonardo da Vinci and Sir Isaac Newton (ref. 12). However, it was Young (ref. 13) who first established the theory by demonstrating how the principles of surface tension and contact angle can be used to explain a great many capillary phenomena. The theory was put on a firm mathematical foundation by Laplace (ref. 14) and later Poisson (ref. 15). Further developments were made by Gauss (ref. 16), who applied the principle of conservation of energy to the system and obtained not only the equation of the free surface but also the conditions of the contact angle. Other earlier investigators include Dupré (ref. 17), Rayleigh (ref. 18), Gibbs (ref. 19), and Plateau (ref. 20), who utilized soap bubbles and other devices to determine the equilibrium configuration of liquids. Later investigations were carried out by Langmuir (ref. 21) and Harkins (refs. 22 and 23) in this country and Adam (ref. 24) and Burdon (ref. 25) in England. In recent times, surface phenomena have been studied by many workers, as attested to by the great wealth of data on the subject (refs. 26 to 48). Some of these investigations have concentrated primarily on contact angle (refs. 35 to 42), while others have devoted themselves to wetting and spreading (refs. 43 to 48).

Liquid Contact Angle

Consider a liquid in contact with a solid surface. The free surface energies at the solid-liquid-vapor interfaces may be represented by the surface-tension forces acting in the direction of the surfaces (ref. 49). The angle at which the liquid meets the solid surface, measured in the liquid, is the contact angle. A schematic diagram illustrating how these surface-tension forces act at the solid-liquid-vapor interfaces is presented in figure 1.

For the liquid to be in equilibrium with the solid surface, the surface-tension forces at the solid-liquid-vapor interfaces must be in balance parallel to the solid surface. Therefore,

$$\sigma_{vs} = \sigma_{ls} + \sigma_{vl} \cos \theta \tag{1}$$

and

$$\theta = \cos^{-1} \frac{\sigma_{vs} - \sigma_{ls}}{\sigma_{vl}} \tag{2}$$

where σ_{vs}, σ_{ls}, and σ_{vl} are the surface tensions of the vapor-solid, liquid-solid, and vapor-liquid interfaces, respectively, and θ is the contact angle. It is observed that the contact angle θ depends on the

magnitudes of the three surface-tension forces. When $(\sigma_{vs} - \sigma_{ls})/\sigma_{vl}$ is between 0 and 1, the contact angle θ will lie between 0° and 90°. When the contact angle θ lies between 0° and 90°, a common convention is to call the liquid a wetting liquid. If, however, $(\sigma_{vs} - \sigma_{ls})/\sigma_{vl}$ lies between 0 and -1, the contact angle θ will lie between 90° and 180°, and the liquid is said to be a nonwetting liquid.

From these considerations, it can be concluded that the contact angle should remain constant in any gravity field, including a weightless environment, because the intermolecular forces that are exhibited in the surfact-tension forces are independent of the level of the gravity field.

Zero-Gravity Liquid Configuration

From many observations of natural phenomena, it can be generally concluded that, when all the external forces on a system are removed, the system will tend toward a state of minimum energy. Hence, when the restraint of gravity is removed from a tank containing a wetting' or a nonwetting liquid (i.e., when the tank is in a weightless environment), this system will tend toward a state of minimum energy. Under these conditions, the contact angle and the tank geometry must be taken into account in order to determine the equilibrium liquid configuration.

Consider a spherical tank partially filled with a wetting liquid where the contact angle θ is greater than 0° but less than 90°. When in a weightless environment, the equilibrium liquid configuration will be a constant-curvature liquid-vapor surface meeting the wall at the same contact angle as was observed in the gravity field. Sketches showing the configuration of a wetting liquid in a spherical tank under the influence of a gravity field and during weightlessness are presented in figure 2. In the case of a spherical tank partially filled with a nonwetting liquid where the contact angle is greater than 90° but less than 180°, the equilibrium liquid configuration in a weightless environment is again a constant-curvature liquid-vapor surface meeting the tank wall at the same contact angle as was observed in the gravity field. Sketches showing the configuration of a nonwetting liquid in a spherical tank under the influence of a gravity field and during weightlessness are presented in figure 3.

In the case of a totally wetting liquid in a spherical tank, that is, a liquid with a contact angle of 0°, the condition of a constant-curvature liquid-vapor surface occurs only when the tank walls are completely wetted and the vapor forms a bubble in the interior of the liquid. The surface energy of the bubble will then tend toward a minimum, which is obtained by minimizing the surface areas of the bubble

(ref. 1). It can be concluded, therefore, that the equilibrium liquid configuration for a totally wetting liquid in a spherical tank when placed in a weightless environment is a completely wetted tank wall with a spherical vapor bubble in the interior of the liquid. A sketch showing the configuration of a totally wetting liquid in a spherical tank under the influence of a gravity field and during weightlessness is presented in figure 4.

Similarly, for a totally nonwetting liquid in a spherical tank, that is, a liquid with a contact angle of 180°, the condition of a constant-curvature liquid-vap ꞌ surface occurs only when the liquid is completely detached from the tank walls. The surface energy of the liquid will tend toward a minimum with a simultaneous reduction of the liquid-vapor surface area. It can be concluded, therefore, that the equilibrium liquid configuration for a totally nonwetting liquid in a spherical tank in a weightless environment is a spherical liquid mass completely detached from the tank walls. The tank walls will be covered by a vapor blanket. A sketch showing the configuration of a totally nonwetting liquid in a spherical tank under the influence of a gravity field and during weightlessness is presented in figure 5.

In this report no attempt is made to give a detailed account of the exact manner in which a liquid migrates from the 1-g configuration to the weightless configuration. At present the basic mechanism of this transition is not well defined. However, one possible explanation is that nonuniform pressure forces, due to nonuniform surface curvature, acting on the liquid-vapor surface of the liquid initiate the transition.

APPARATUS AND PROCEDURE

Among the several methods available for producing a weightless environment (see ref. 50), one of the most direct is to allow a test body to undergo a free fall. During the time of free fall, the test body will be in true weightlessness, as there are no restraining forces acting on it.

Test Facility

In the present investigation a weightless environment was obtained in a drop tower with a usable drop height of 85 feet that yeilds a free-fall time of 2.3 seconds. This tower is the 21-foot-square, eight-story structure shown in figures 6 and 7. In this particular facility air drag on the experimental package is kept to a minimum by allowing the experimental package to fall within a protective drag shield. The

experimental package and the drag shield were unguided during the free
fall. A schematic diagram of the experimental package and drag shield
is shown in figure 8.

A 3- by 5- by 6.75-foot-deep sandbox was located on the first floor
of the building and served as part of a deceleration device for the ex-
periment. Adjacent to the sandbox was a sand storage hopper, which was
used in aerating the sand. Sand aeration was accomplished by using an
enclosed screw-type auger to pump sand from the sandbox into the hopper
and then back into the sandbox through a strainer.

The fifth floor of the drop tower served as a working and assembly
area for handling the experiment before and after a test drop. In order
to facilitate test operations, a cradle support for the drag shield was
welded to a movable section of floor that could be rolled out of the way
before each drop.

The eighth floor contained an electrically powered hoist used for
lifting the experiment to its predrop position. Attached to a roof
beam directly over the drop area was a combination wire support and re-
lease mechanism from which the experiment was hung. The release mecha-
nism consisted of a double-acting air cylinder with a hard steel knife
edge attached to the piston. Pressurization of the air cylinder forced
the knife edge to cut the wire against an anvil, thereby ensuring a
smooth release.

Drag Shield

Air resistance on the experiment package was kept below 10^{-5} g of
deceleration by allowing the experimental package to fall within a 400-
pound drag shield. The ratio of weight to frontal area of the drag
shield was kept high so that the deviation from a true free fall would
be kept to a minimum. Both drag shield and experiment package fell to-
gether during the test drop. Access to the inside of the drag shield
was through two detachable side plates. Three maple spikes, 3 inches
in diameter and 73 inches in length, were mounted in a row along the
bottom. These served to decelerate the drag shield and the experiment
package upon impact into the sandbox. Attached to the bottom of the
spikes were machined aluminum tips. The size of the aluminum tips was
reduced after every drop to compensate for sand packing and thus main-
tain a nominal decelerating force on the experiment of 15 g's.

Experiment Package

The fluid under investigation was contained in a spherical glass
tank suitably mounted and illuminated to allow a high-speed motion-
picture camera to photograph the entire tank during free fall. The

experimental package is shown in figure 9. The tanks used were standard, round-bottomed, Pyrex flasks varying in size from 34 to 1068 milliliters. The tanks were mounted so that the neck was in the up position for the nonwetting-liquid experiments and in the down position for the wetting-liquid experiments. It was found that the presence of the neck had no effect on the weightless configuration of the liquid. A 16-millimeter Fairchild high-speed camera with a 100-foot film capacity was used to obtain the photographic data. Average film speed was 400 frames per second, which gave a total running time of 10 seconds. Illumination of the spherical tanks was provided by four 20-watt, 28-volt, direct-current light bulbs. In order to keep highlights and glare to a minimum, the tanks were mounted inside a light box having a dull white interior finish, and the light bulbs were arranged to provide indirect lighting. A photograph of a sphere containing mercury and mounted in place is shown in figure 10. Electrical power for the lights and camera was carried in the experiment package and consisted of 48 nickel-cadmium cells stacked into four batteries of 12 cells each. Three batteries powered the lights, and one battery powered the camera. The lighting circuit was connected by means of a relay to the camera control circuit so that lights and camera turned off after film ran through the camera.

Test Liquids

The liquids used in this experimental investigation were triple-distilled mercury, 200-proof ethyl alcohol, distilled water, and chemically pure carbon tetrachloride. The bulk of the experimental data was obtained using mercury as being representative of a nonwetting liquid and ethyl alcohol as being representative of a totally wetting liquid. Limited data were obtained with water and carbon tetrachloride, both of which are totally wetting liquids. The properties of these liquids are given in the following table:

	Mercury	Ethyl alcohol	Water	Carbon tetrachloride
Density at 20° C, g/cm^3	13.546	0.7893	0.9982	1.595
Viscosity at 20° C, centipoises	1.554	1.200	1.005	1.038 at 15° C
Surface tension at 20° C in air, dynes/cm	476.1	22.3	72.75	26.8
Density/surface tension, sec^2/cm^3	0.0284	0.0354	0.0137	0.0596

During the experimental investigation, the test liquids were at essentially ambient pressure and temperature. The liquid-vapor interface in every case was liquid to air. In the investigation of alcohol, a small amount of blue dye (spirit blue) was added to improve the photographic quality. The addition of the dye did not have any measurable effect on the surface tension of the alcohol.

Operating Procedure

Before each test drop the spherical tanks were carefully cleaned with a detergent solution and then with a chromic acid solution, rinsed in cold running water and then in distilled water, and finally dried over a Bunsen flame. All glassware such as graduate cylinders, funnels, or pipettes that came into contact with the test liquid were cleaned in the same manner. After cleaning, the spherical tanks were filled with the proper amount of test liquid by means of a graduate cylinder.

A timing trace using 60-cycle-per-second line current was made with the camera before and after every second drop. A plot of the frame number against time was later made and used to obtain equilibrium times for the test fluids. This method resulted in a measurement of time to an accuracy of 2 percent of the total equilibrium time.

At the start of a test drop the experiment package was statically balanced with brass weights, loaded into the drag shield, and hoisted to the eighth floor. A 1-foot length of wire clamped between two hardened steel blocks was used to support the experiment package and drag shield from the wire release mechanism. A photograph of the experiment package hanging inside and supporting the drag shield is shown in figure 11. Both side plates were attached and the hoist cables released. In order to ensure quiescent initial conditions, sufficient time was allowed for the disturbances in the test liquid to damp out. The camera and lights were started by breaking an external connection; they were allowed to run for 5 seconds before the actual drop.

During the drop both experiment and drag shield fell together. Immediately before impact into the sandbox, air resistance had slowed the drag shield to the point where the experiment package had caught up to it, and the experiment package rested on the bottom of the drag shield. Since the experiment package had contacted the bottom of the drag shield before impact into the sandbox, the time in weightlessness was 1.95 seconds.

RESULTS AND DISCUSSION

The experimental results of this investigation are presented in the form of selected photographs taken from the motion-picture data obtained

during each test drop. The liquid configuration both in a 1-g environment and in a weightless environment is discussed together with the manner of transition of the liquid from the 1-g configuration to the zero-g configuration. In addition, the effects of such parameters as tank size and amount of liquid in the tank on the equilibrium liquid configuration during weightlessness are evaluated.

Configuration of Mercury

The results of the experimental investigation of mercury in spherical glass tanks are presented in figures 12 to 22 in the form of selected photographs taken from the motion-picture data obtained during each test drop. The results obtained in the 34-, 54-, 200-, 500-, and 1068-milliliter glass spheres are presented in figures 12 to 16. For each of these sizes of spheres and for each ratio of liquid to tank volume investigated, two photographs are presented. The first photograph shows the liquid configuration prior to being subjected to zero gravity. The second photograph presents the equilibrium liquid configuration when exposed to a zero-gravity environment. It should be noted that complete stability was not achieved in all test drops; hence, the photographs showing the equilibrium configuration of the liquid were selected as the liquid was oscillating about this configuration. The results obtained from the 100-milliliter glass spheres are presented in figures 17 to 22. These figures present a sequence of photographs after 0, 0.2, 0.4, 0.6, 0.8, 1.0, 1.5, and 1.95 seconds of exposure to zero gravity for six ratios of liquid to tank volume. It should be noted that in some of the figures the same size tank appears as two different sizes. This resulted from a change in the camera lens size during the experimental program.

It can be seen that at 1 g the mercury rests in a pool at the bottom of the sphere. The liquid-vapor surface of the mercury is essentially flat. At low ratios of liquid to tank volume a convex meniscus was observed as shown in figures 13(a) to (c). The measured contact angle of the mercury with the glass spheres used in this investigation was of the order of 125°. As the amount of mercury in the sphere was increased, the height of the meniscus decreased because of the curvature of the wall, so that when the sphere was approximately 80 percent full, no meniscus existed. Typical photographs of the 80-percent-full sphere are shown in figures 14(f), 15(f), and 21. As the liquid- to tank-volume ratio was increased above 80 percent, the meniscus became concave as shown schematically in figure 3(d). It should be noted that, regardless of the amount of mercury in the spheres, the contact angle remained unchanged; the variation in the height and direction of the meniscus is a function of the curvature of the tank walls.

Effect of volume ratio. - The stable equilibrium liquid configuration for mercury in spherical glass tanks in a weightless environment is one in which the liquid-vapor surface of the mercury is a surface of constant curvature and the mercury remains in contact with the walls of the sphere at the same contact angle as was observed in the 1-g environment. This equilibrium liquid configuration compares favorably with the predicted configuration shown in figure 3. At liquid- to tank-volume ratios less than 80 percent, the stable equilibrium liquid configuration is such that the liquid-vapor surface of the mercury is a spherical segment (figs. 12 to 16). At a liquid- to tank-volume ratio of 80 percent, the liquid-vapor surface of the mercury is flat (i.e., a surface of infinite radius, see figs. 14(f) and 15(f)). At volume ratios in excess of 80 percent the liquid-vapor surface is again a spherical segment; however, it is inverted with respect to that observed at fillings below 80 percent. The results of a test drop with a 97-percent-full sphere are shown in figure 22. Because of the nontransparency of mercury, the concave meniscus is not seen in this sequence of photographs. It can be concluded from the above results that the shape of the liquid-vapor surface in spherical tanks is dictated by the contact angle of the liquid and the constant-surface-curvature configuration, and that the contact angle is unaffected by the level of the gravity field.

Effect of tank size. - The equilibrium liquid configuration during weightlessness appears to be unaffected by the tank size over the range of sizes investigated (figs. 12 to 22).

Time history. - The manner in which the mercury migrates from the 1-g configuration to the zero-gravity equilibrium liquid configuration is shown in figures 17 to 22. As discussed previously, at zero gravity, nonuniform pressure forces acting on the liquid-vapor surface of the mercury because of nonuniform surface curvature cause the liquid to move down the walls of the tank. As a result of liquid inflow to the center of the liquid-vapor surface, the liquid in that region moves upward. The liquid mass then oscillates about the equilibrium liquid configuration until viscous forces in the liquid damp out the oscillations and bring the liquid to rest (see figs. 17, 19, 20, and 21). It should be noted that, in the case of the 80-percent-full sphere (fig. 21), the zero-gravity equilibrium liquid configuration is identical to the 1-g configuration; hence no liquid motion is observed when the sphere is placed in zero gravity.

It can be seen from figure 18 that there are times when the mercury completely leaves the tank walls. In these cases it is felt that the kinetic energy of the liquid resulting from the motion of the mercury down the tank walls causes an overshoot of the zero-gravity equilibrium configuration of sufficient magnitude to break the mercury loose from the tank walls. The mercury, upon leaving the walls and under the

action of surface tension, becomes spherical. This spherical mass of mercury leaves the wall with a small velocity, which causes it to impinge on the opposite wall of the tank. It is felt that after impingement and dissipation of energy the mercury assumes the stable equilibrium liquid configuration.

Configuration of Alcohol

The results of the experimental investigation of ethyl alcohol in spherical glass tanks are shown in figures 23 to 33 in the form of selected photographs taken from the motion-picture data obtained during each test drop. The results obtained in the 54-, 200-, 500-, and 1068-milliliter glass spheres are presented in figures 23 to 26. For each of these sizes of spheres and for each value of liquid- to tank-volume ratio investigated, three photographs are presented. The first photograph shows the liquid configuration prior to being subjected to zero gravity. The second shows the liquid as it is approaching its equilibrium configuration. The third gives the liquid configuration after equilibrium is reached. The results obtained from the 100-milliliter glass spheres are presented in figures 27 to 33. These figures present a sequence of photographs during the 1.95-second period of weightlessness showing, generally, the approach to equilibrium and the liquid configuration after equilibrium is reached.

It can be seen from figures 23 to 33 that, at 1-g, the alcohol rests in a pool at the bottom of the sphere. The liquid-vapor surface is essentially flat. The meniscus is concave in all cases, and the liquid contacts the wall at an angle of 0°.

Effect of volume ratio. - The zero-gravity equilibrium liquid configuration for ethyl alcohol in spherical glass tanks at every liquid-to tank-volume ratio investigated is a completely wetted tank wall with a spherical vapor bubble in the interior of the liquid. This configuration corresponds to the predicted configuration shown in figure 4. The second photograph for each liquid- to tank-volume ratio in figures 23 to 26 shows the alcohol at the moment of total wetting.

Effect of tank size. - For each experimental test drop, a measure was made of the total time required for the alcohol to wet the walls of the spherical tanks completely. A plot of the total time required for complete wetting against the amount of liquid in the tank for the five tank sizes investigated is given in figure 34. The variation of total time to complete wetting with linear surface distance above the initial liquid level (i.e., total linear distance to be wetted) is presented in figure 35. Examination of these figures reveals that the time required to wet the tank walls completely increases as the volume of the tank

increases and decreases as the amount of liquid in a given tank increases. Typical times for total wetting to occur for a volume ratio of 70 percent were 0.52 and 1.76 seconds for the 54- and 1068-milliliter tanks, respectively.

Time history. - The manner in which the alcohol migrates from the 1-g configuration to the zero-g equilibrium liquid configuration is shown in figures 27 to 33. Upon exposure to zero gravity the alcohol rises up the tank wall until total wetting has occurred. The vapor bubble can be observed to oscillate about the spherical configuration.

Effect of Liquid Properties

In order to determine what effect liquid properties had on the time to wet the tank walls completely, two test drops were made in which three 100-milliliter glass spheres, each containing a different liquid, were mounted in the experimental test package. Three totally wetting liquids were used, carbon tetrachloride, ethyl alcohol, and water. These liquids were choosen because they have nearly the same viscosity but different density and surface tension (see table of liquid properties). The photographic results obtained from these two drops are presented in figures 36 and 37. These two sequences of photographs reveal that water, which has the lowest density to surface-tension ratio, completely wetted the tank walls in the shortest time, while carbon tetrachloride, which has the largest density to surface-tension ratio, required the longest time. The total time to wet the tank walls completely is plotted against the liquid- to tank-volume ratio in figure 38. These results agree with the analysis of Benedikt (see ref. 2), which indicated that the time to reach equilibrium is directly proportional to the square root of the density to surface-tension ratio.

SUMMARY OF RESULTS

The experimental investigation of the equilibrium liquid configuration of typical wetting and nonwetting liquids in spherical glass tanks in a weightless environment yielded the following results:

1. The stable equilibrium liquid configuration for mercury in spherical glass tanks in a weightless environment was one in which the liquid-vapor surface was a surface of constant curvature and the mercury remains in contact with the tank walls at the same contact angle as was observed in the 1-g environment.

2. The zero-gravity equilibrium liquid configuration of mercury appears to be unaffected by tank size.

E-1484

3. The equilibrium configuration of mercury was affected by the liquid- to tank-volume ratio to the extent that at volume ratios below 80 percent the liquid-vapor surface was convex and at volume ratios above 80 percent the liquid-vapor surface was concave. At a volume ratio of 80 percent the liquid-vapor surface was flat.

4. The liquid contact angle remained constant at 1 g and at zero g and appeared to be unaffected by the level of the gravity field.

5. The zero-gravity equilibrium configuration for ethyl alcohol in spherical glass tanks was a completely wetted tank wall with a spherical vapor bubble in the interior of the liquid.

6. For carbon tetrachloride, ethyl alcohol, and water, the time required to wet the tank wall completely increased with an increase in the density to surface-tension ratio.

Lewis Research Center
    National Aeronautics and Space Administration
        Cleveland, Ohio, December 4, 1961

REFERENCES

1. Li, Ta: Liquid Behavior in a Zero-G Field. Rep. AE 60-0682, Convair-Astronautics, Aug. 1960.

2. Benedikt, E. T.: Scale of Separation Phenomena in Liquids Under Conditions of Nearly Free Fall. ARS Jour., vol. 29, no. 2, Feb. 1959, pp. 150-151.

3. Benedikt, E. T.: General Behavior of a Liquid in a Zero or Near Zero Gravity Environment. Rep. ASG-TM-60-9Z6, Norair Div., Northrop Corp., May 1960.

4. Benedikt, E. T.: Dynamics of a Liquid Spheroid Under the Action of Cohesive Forces. Rep. ASRL-TM-60-10, Norair Div., Northrop Corp., Sept. 1960.

5. Reynolds, William C.: Behavior of Liquids in Free Fall. Jour. Aero/Space Sci., vol. 26, no. 12, Dec. 1959, pp. 847-848.

6. Usiskin, C. M., and Siegel, R.: An Experimental Study of Boiling in Reduced and Zero Gravity Fields. Paper 60-HT-10, ASME-AIChE, 1960.

14

7. Siegel, Robert: Transient Capillary Rise in Reduced and Zero-Gravity Fields. Paper 60-WA-201, ASME, 1960.

8. Brazinsky, Irving, and Weiss, Solomon: A Photographic Study of Liquid Hydrogen at Zero Gravity. NASA TN D-1107, 1961.

9. Steinle, Hans: Heat Transfer in a Zero-G Field. Convair-Astronautics, 1960.

10. Neiner, J. J.: The Effect of Zero Gravity on Fluid Behavior and System Design. TN 59-149, WADC, Apr. 1949.

11. Sherley, Joan: Evaluation of Liquid Behavior in a Zero-G Field Using Free Floating Technique. Convair-Astronautics, 1960.

12. Yust, Walter, ed.: Surface Tension. Encyclopaedia Britannica, Inc., vol. 21, 1947, pp. 593-602.

13. Young, Thomas: Essay on the Cohesion of Fluids. Roy. Phil. Trans., Dec. 20, 1805, pp. 65-87.

14. Laplace, Pierre Simon: Mecanique Celeste, Supplement to Tenth Book, 1806.

15. Poisson, Simeon Denis: Nouvelle Theorie de L'Action. 1831.

16. Gauss, Carl Friederich: Principia Generalia Theoriae Figurae Fluidorum in Statu Aequilibrii. Gottingen, 1830.

17. Dupre, Athanase: Memoirs of the Mechanical Theory of Heat. Nos. 5, 6, and 7, Ann. Chim. et Phys., 1866-1868.

18. Rayleigh: Collected Scientific Papers. Vol. VI. Cambridge Univ. Press (London), 1920.

19. Gibbs, J. Willard: Collected Works. Vol. 2. Longmans, Green, and Co., 1928.

20. Plateau, J. A. F.: Statique Experimentale et Theorique des Liquides. 1873.

21. Langmuir, Irving: The Constitution and Fundamental Properties of Solids and Liquids, I. Jour. Am. Chem. Soc., vol. 38, no. 11, Nov. 1916, pp. 2221-2295.

22. Harkins, William D., and Loeser, E. H.: Surfaces of Solids. XIX. Molecular Interactions Between Metals and Hydrocarbons. Jour. Chem. Phys., vol. 18, no. 4, Apr. 1950, pp. 556-560.

23. Harkins, William D.: The Physical Chemistry of Surface Films. Reinhold Pub. Corp., 1952.

24. Adam, Neil Kensington: The Physics and Chemistry of Surfaces. Oxford Univ. Press, 1941.

25. Burdon, R. S.: Surface Tension and the Spreading of Liquids. Cambridge Univ. Press (London), 1940.

26. Fowkes, Frederick M., and Harkins, William D.: The State of Monolayers Adsorbed at the Interface Solid-Aqueous Solution. Jour. Am. Chem. Soc., vol. 62, no. 12, Dec. 1940, pp. 3377-3386.

27. Gurney, C.: Surface Forces in Liquids and Solids. Proc. Phys. Soc. (London), sec. A, no. 358, vol. 62, Oct. 1, 1949, pp. 639-648.

28. Koenig, Frederick O.: On the Thermodynamic Relation Between Surface Tension and Curvature. Jour. Chem. Phys., vol. 18, no. 4, Apr. 1950, pp. 449-459.

29. Shuttleworth, R.: The Surface Tension of Solids. Proc. Phys. Soc. (London), sec. A, vol. 63, no. 365, May 1, 1950, pp. 444-457.

30. Alexander, A. E.: Surface Chemistry. Longmans, Green, and Co., 1951.

31. Partington, J. R.: An Advanced Treatise on Physical Chemistry. Vol. II. Longmans, Green, and Co., 1951, pp. 134-207.

32. Yarnold, G. D.: Understanding Surface Tension. Contemporary Phys., vol. 1, no. 4, Apr. 1960, pp. 267-275.

33. Adamson, Arthur W.: Physical Chemistry of Surfaces. Intersci. Pub., 1960.

34. Goodrich, F. C.: The Mathematical Theory of Capillarity, I; II; III. Proc. Roy. Soc. (London), ser. A, vol. 260, no. 1303, Mar. 21, 1961, pp. 481-509.

35. Scholberg, Harold M., and Wetzel, W. W.: Some Observations on the Theory of Contact Angles. Jour. Chem. Phys., vol. 13, no. 10, Oct. 1945, p. 448.

36. Cassie, A. B. D.: Contact Angles. Discussions of Faraday Soc., no. 3, 1948, pp. 11-16.

37. Gregg, S. J.: Hystersis of the Contact Angle. Jour. Chem. Phys., vol. 16, no. 5, May 1948, pp. 549-550.

16

38. Yarnold, G. D., and Mason, B. J.: A Theory of the Angle of Contact. Proc. Phys. Soc., sec. B, vol. 62, pt. 2, Feb. 1949, pp. 121-125.

39. Yarnold, G. D., and Mason, B. J.: The Angle of Contact Between Water and Wax. Proc. Phys. Soc., sec. B, vol. 62, pt. 2, Feb. 1949, pp. 125-128.

40. Bikerman, J. J.: Surface Roughness and Contact Angle. Jour. Phys. and Colloid Chem., vol. 54, no. 5, May 1950, pp. 653-658.

41. McNutt, James E., and Andes, George M.: Relationship of the Contact Angle to Interfacial Energies. Jour. Chem. Phys., vol. 30, no. 5, May 1959, pp. 1300-1303.

42. Good, Robert J., and Girifalco, L. A.: A Theory for Estimation of Surface and Interfacial Energies. III. Estimation of Surface Energies of Solids from Contact Angle Data. Jour. Phys. Chem., vol. 64, no. 5, May 1960, pp. 561-565.

43. Bartwell, F. E.: Wetting of Solids by Liquids. Colloid Chem., vol. III, Chem. Catalog Co., Inc., 1931.

44. Washburn, E. Roger, and Anderson, Elmer A.: The Pressure Against Which Oils Will Spread on Solids. Jour. Phys. Chem., vol. 50, no. 5, Sept. 1946, pp. 401-406.

45. Miller, N. F.: The Wetting of Steel Surfaces by Esters of Unsaturated Fatty Acids. Jour. Phys. Chem., vol. 50, no. 4, July 1946, pp. 300-319.

46. Shuttleworth, R., and Bailey, G. L. J.: The Spreading of a Liquid Over a Rough Solid. Discussions of Faraday Soc., no. 3, 1948, pp. 16-21.

47. Bernett, M. K., and Zisman, W. A.: Relation of Wettability by Aqueous Solutions to the Surface Constitution of Low-Energy Solids. Jour. Phys. Chem., vol. 63, no. 8, Aug. 1959, pp. 1241-1246.

48. Shafrin, Elaine G., and Zisman, William A.: Constitutive Relations in the Wetting of Low Energy Surfaces and the Theory of the Retraction Method of Preparing Monolayers. Jour. Phys. Chem., vol. 64, no. 5, May 1960, pp. 519-524.

49. Glasstone, Samuel: Textbook of Physical Chemistry. Second ed., D. Van Nostrand Co., Inc., 1946, pp. 481-483.

50. Gerathewohl, Siegfried J.: Zero-G Devices and Weightlessness Simulators. Pub. 781, Nat. Acad. Sci.-Nat. Res. Council, 1961.

E-1484
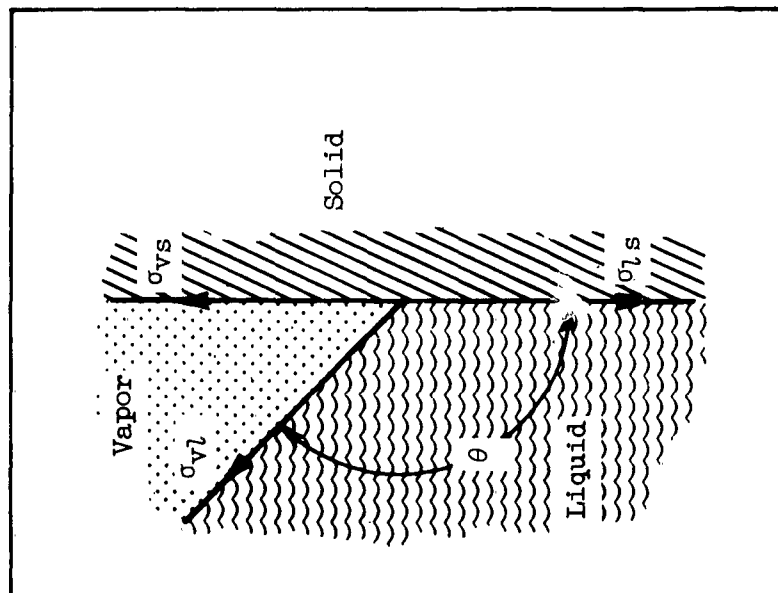
(b) Nonwetting liquid; $90° < \theta < 180°$.

(a) Wetting liquid; $0° < \theta < 90°$.

Figure 1. - Surface-tension forces σ and contact angle θ at solid-liquid-vapor interfaces.
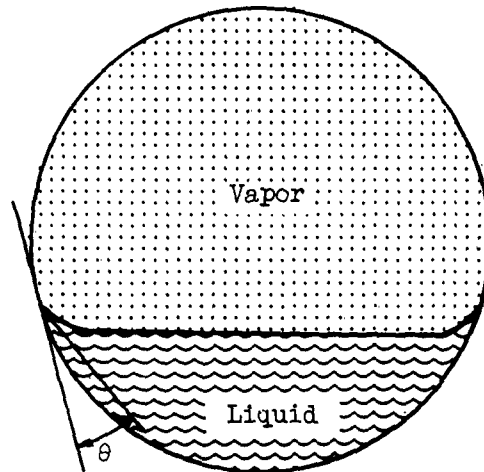
1-g configuration   Zero-g equilibrium configuration
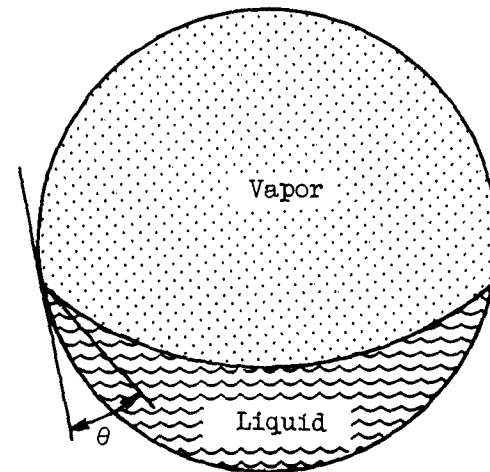
(a) Low liquid- to tank-volume ratios.
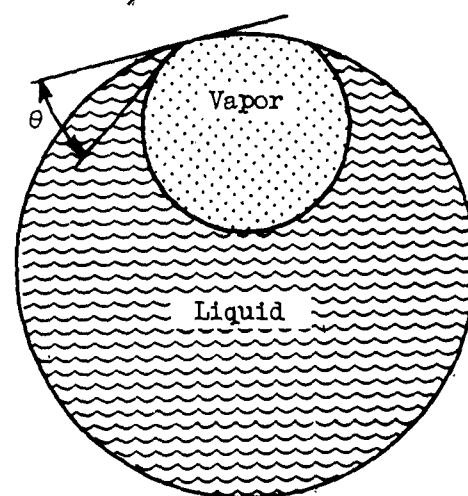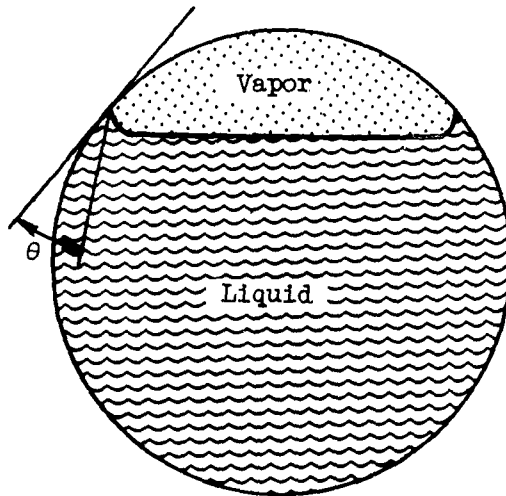
(b) High liquid- to tank-volume ratios.

Figure 2. - Spherical tank partially filled with wetting liquid. Contact
angle: $0^{\circ} < \theta < 90^{\circ}$.

1-g configuration

Zero-g equilibrium
configuration
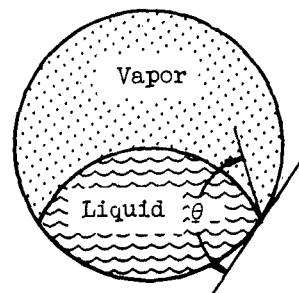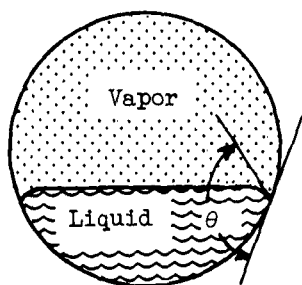
(a) 30 percent full.
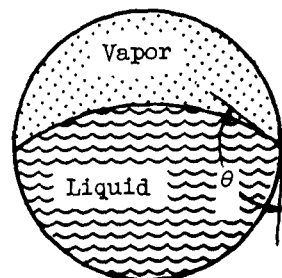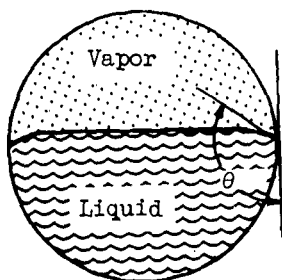
(b) 60 percent full.
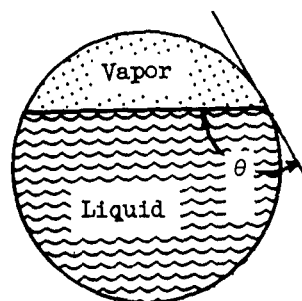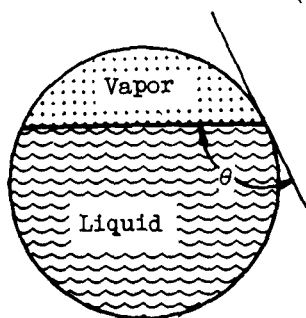
(c) 80 percent full.
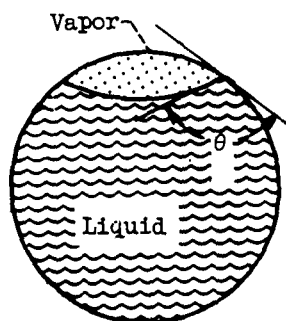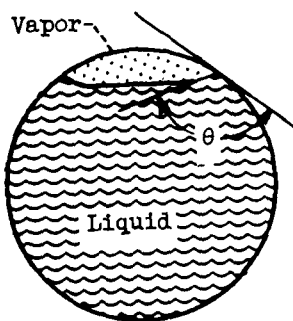
(d) 95 percent full.

Figure 3. - Spherical tank partially filled with nonwetting liq-
uid at different liquid- to tank-volume ratios. Contact angle:
$90^{\circ} < \theta < 180^{\circ}$.
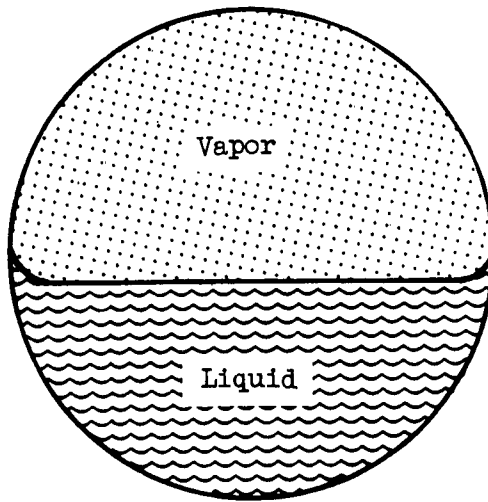
(a) 1-g configuration.
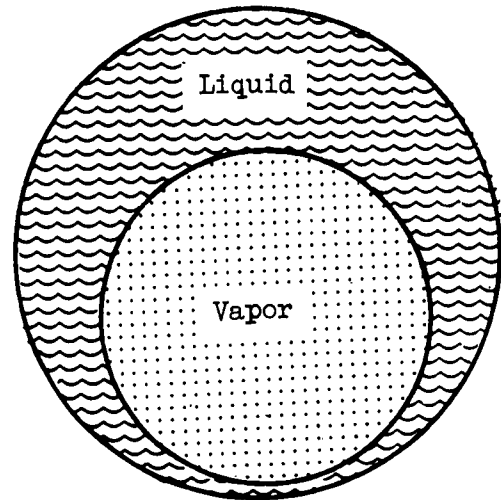
(b) Zero-g equilibrium configuration.

Figure 4. - Spherical tank partially filled with totally wetting liquid. Contact angle θ, 0°.
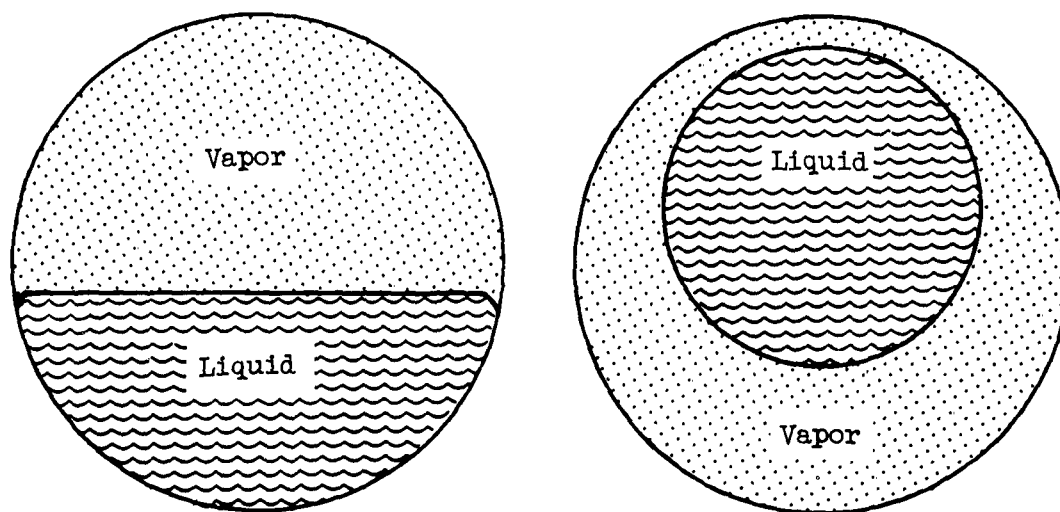
(a) 1-g configuration.

(b) Zero-g equilibrium configuration.

Figure 5. - Spherical tank partially filled with totally nonwetting liquid. Contact angle θ, 180°.

C-57170
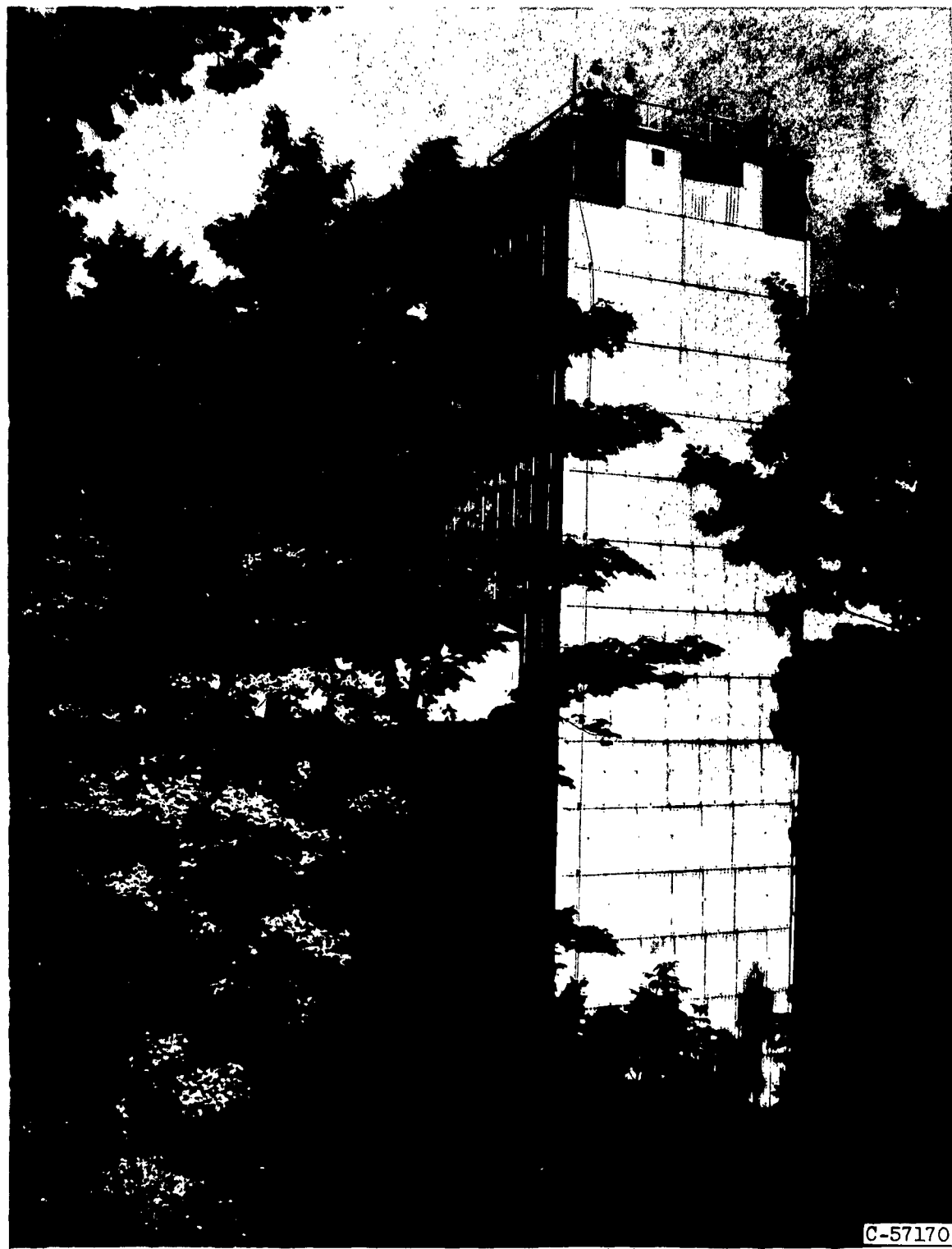
Figure 6. - 100-foot drop tower for simulation of weightlessness.

Wire-release mechanism

Eighth floor:
experiment in
predrop position

Dual-cable hoist for
lifting test package

Sixth floor:
chemical laboratory

Drag shield
support
mounted on
movable floor

Fifth floor:
experiment assembly
and working area

Actual drop
height,
85 ft

Guard rail
(on all floors)

5- by 9-ft hole
(on all floors)

First floor:
$6\frac{3}{4}$ -ft-deep
sandbox

Sand storage hopper
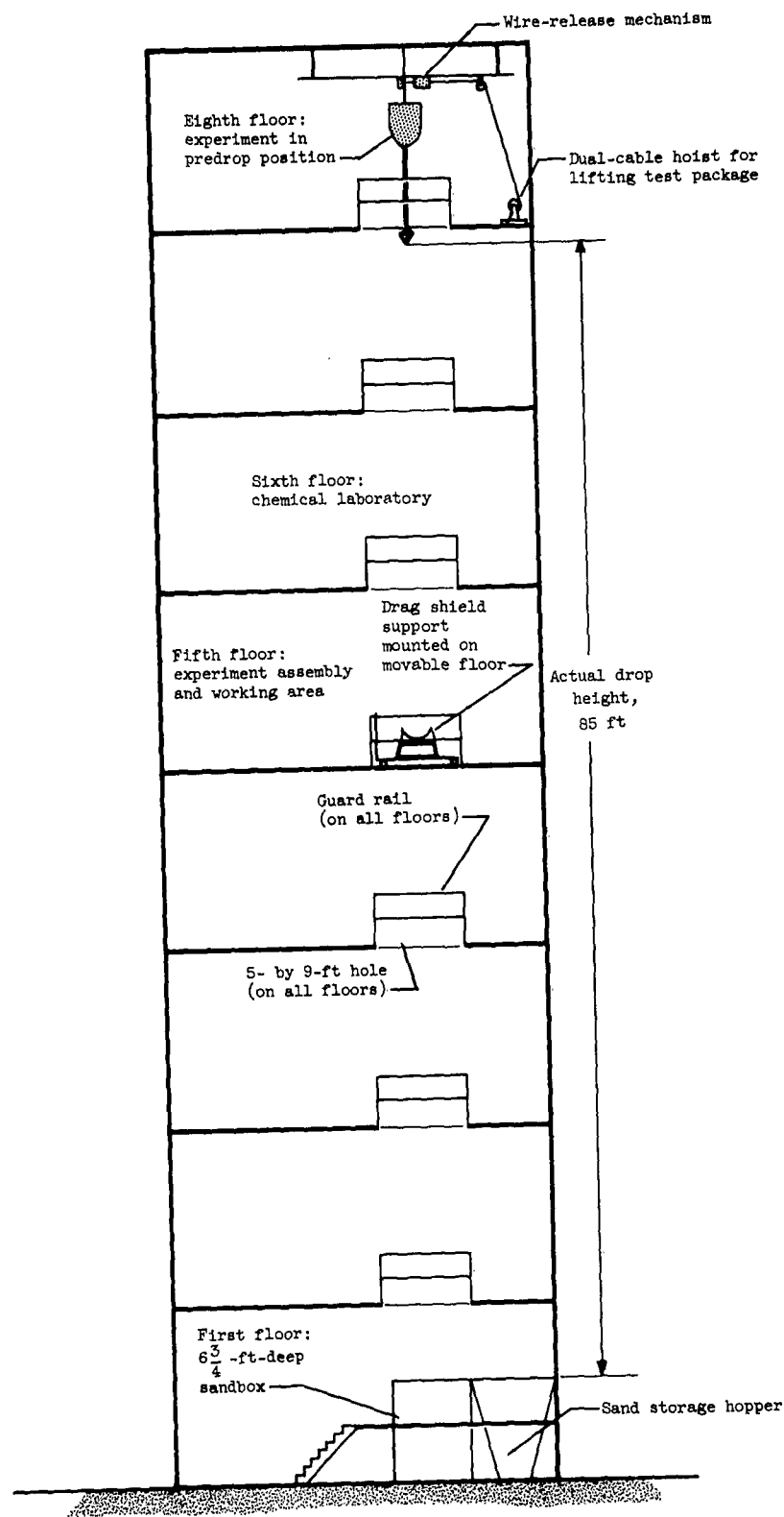
CD-7379

Figure 7. - Schematic drawing of 100-foot drop tower.

Music-wire
support

Wire-release mechanism

Drag shield

Experiment package

8"

Base rounded to
reduce air drag

(a) Before test drop.

(b) During test drop.

CD-7380
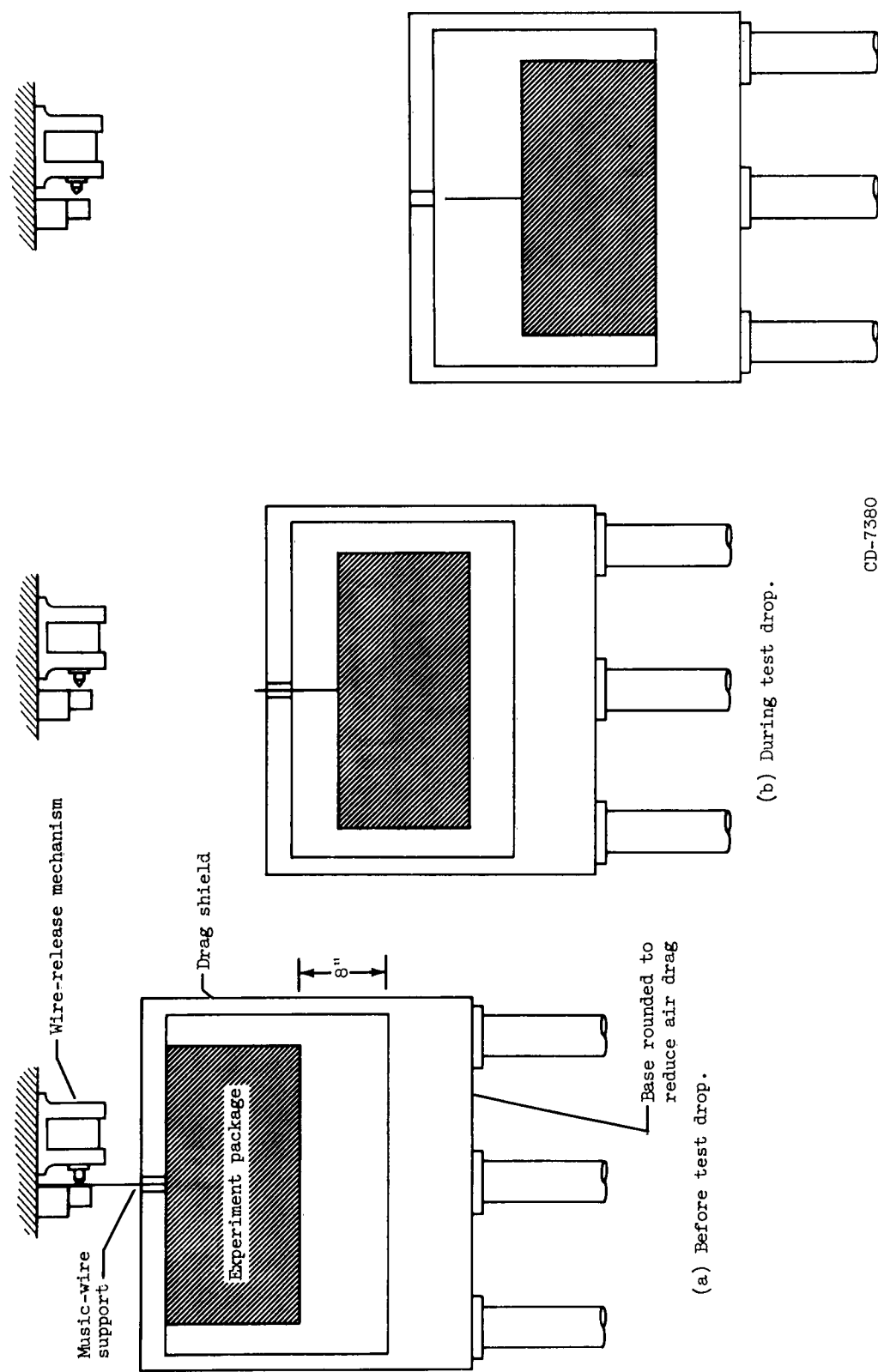
(c) After test drop.

Figure 8. - Schematic drawing showing position of experiment package and drag shield before, during, and after test drop.

E-1484
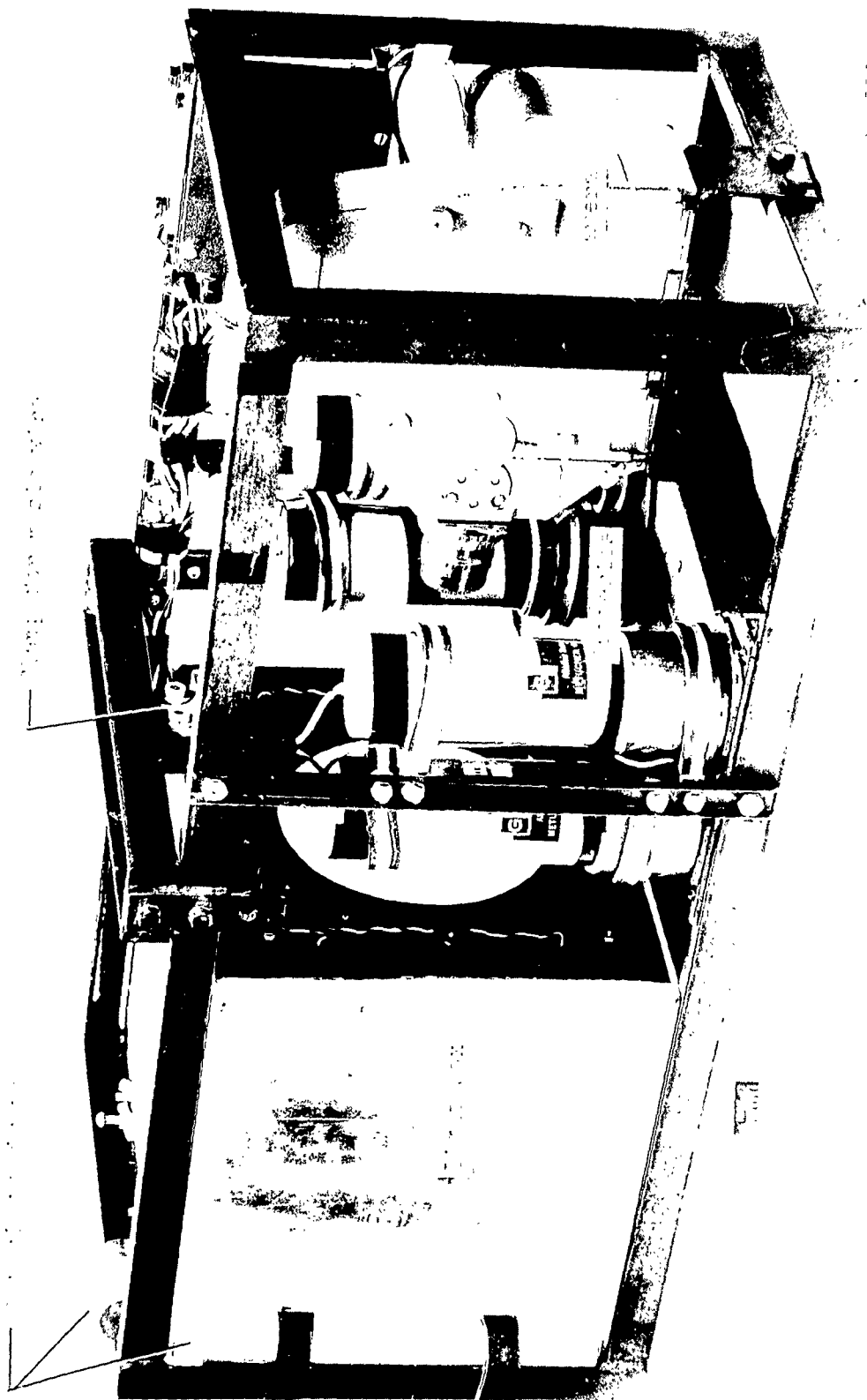
Figure 9. - View of experiment package showing camera, batteries, light box, and balancing weights.
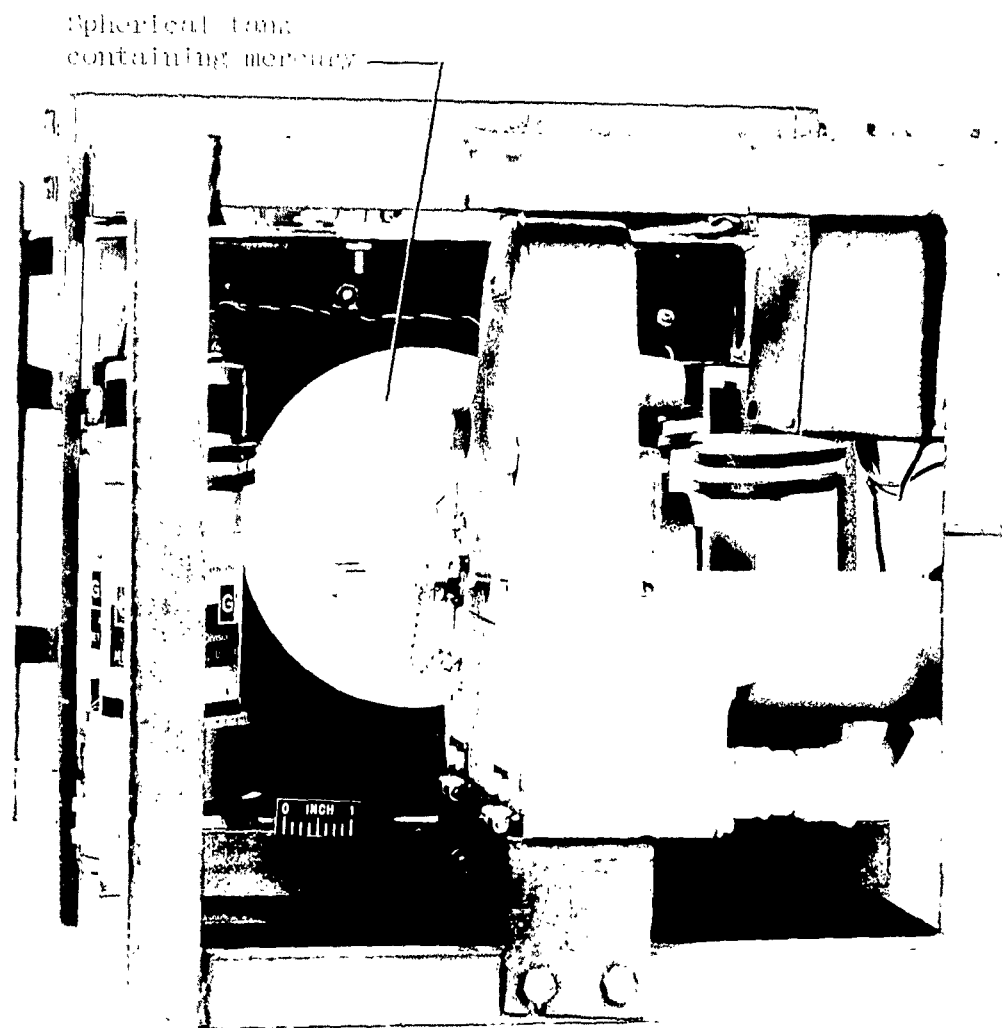
Figure 10. - View of experiment package showing spherical tank containing test liquid mounted inside light box.
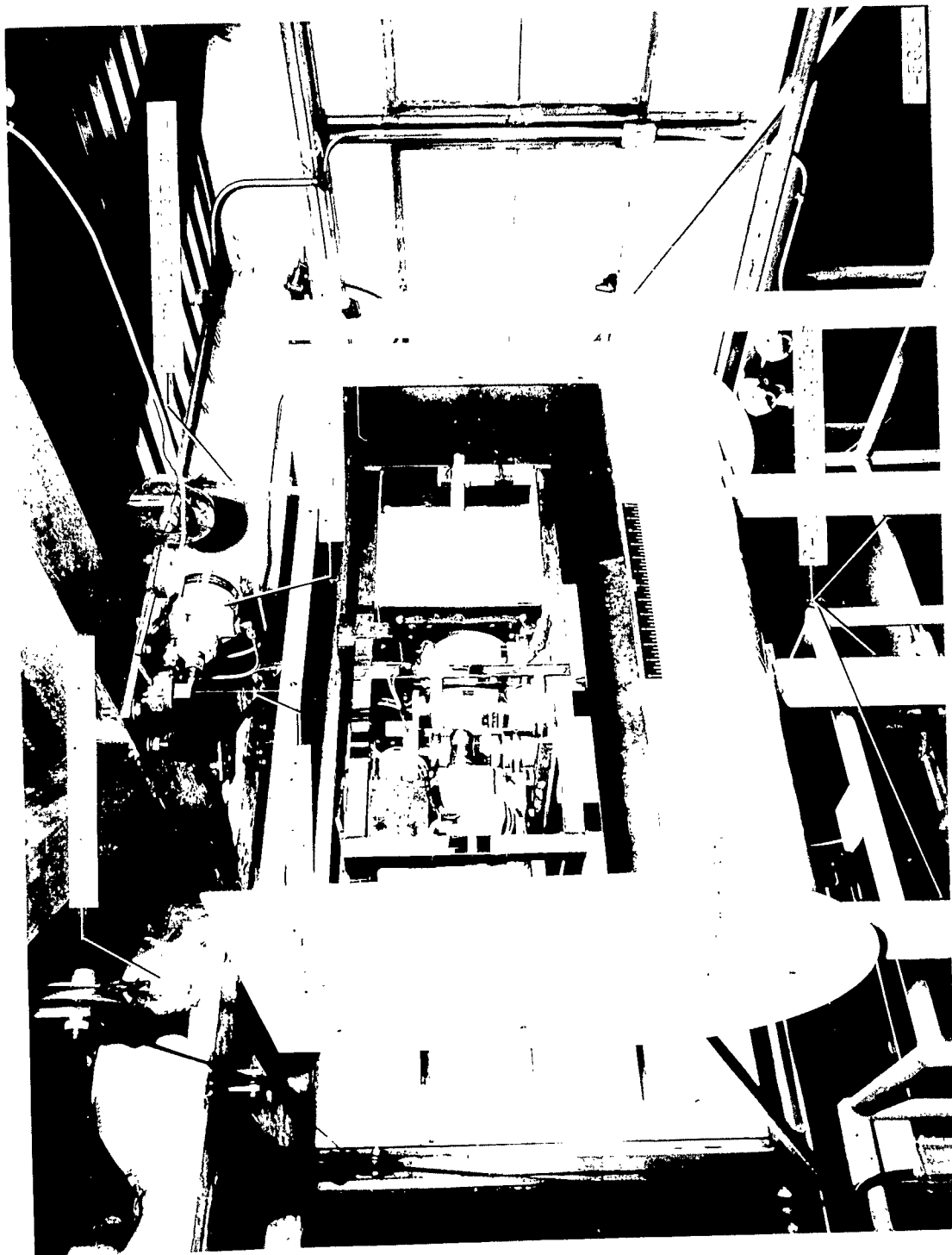
Figure 11. – Experiment package hanging inside drag shield prior to test drop.

28

(a) 3.7 percent full.

(b) 10 percent full.

(c) 14.7 percent full.

(d) 44.1 percent full.

(e) 80.0 percent full.   C-58617
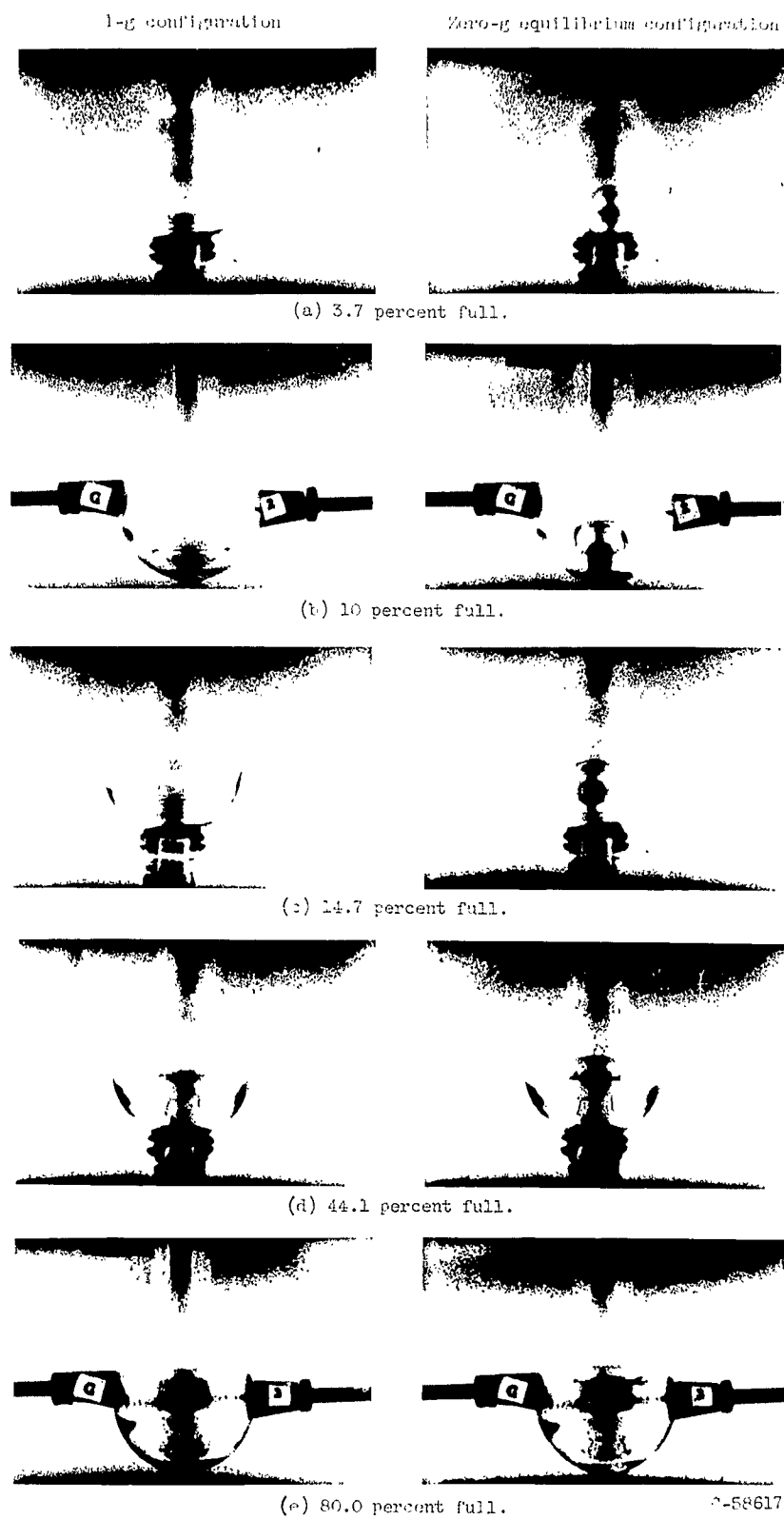
Figure 12. - Mercury in 34-milliliter glass spheres over range of liquid-to tank-volume ratios.

1-g configuration Zero-g equilibrium configuration

(a) 4.6 percent full.

(b) 9.3 percent full.

(c) 18.5 percent full. C-58618
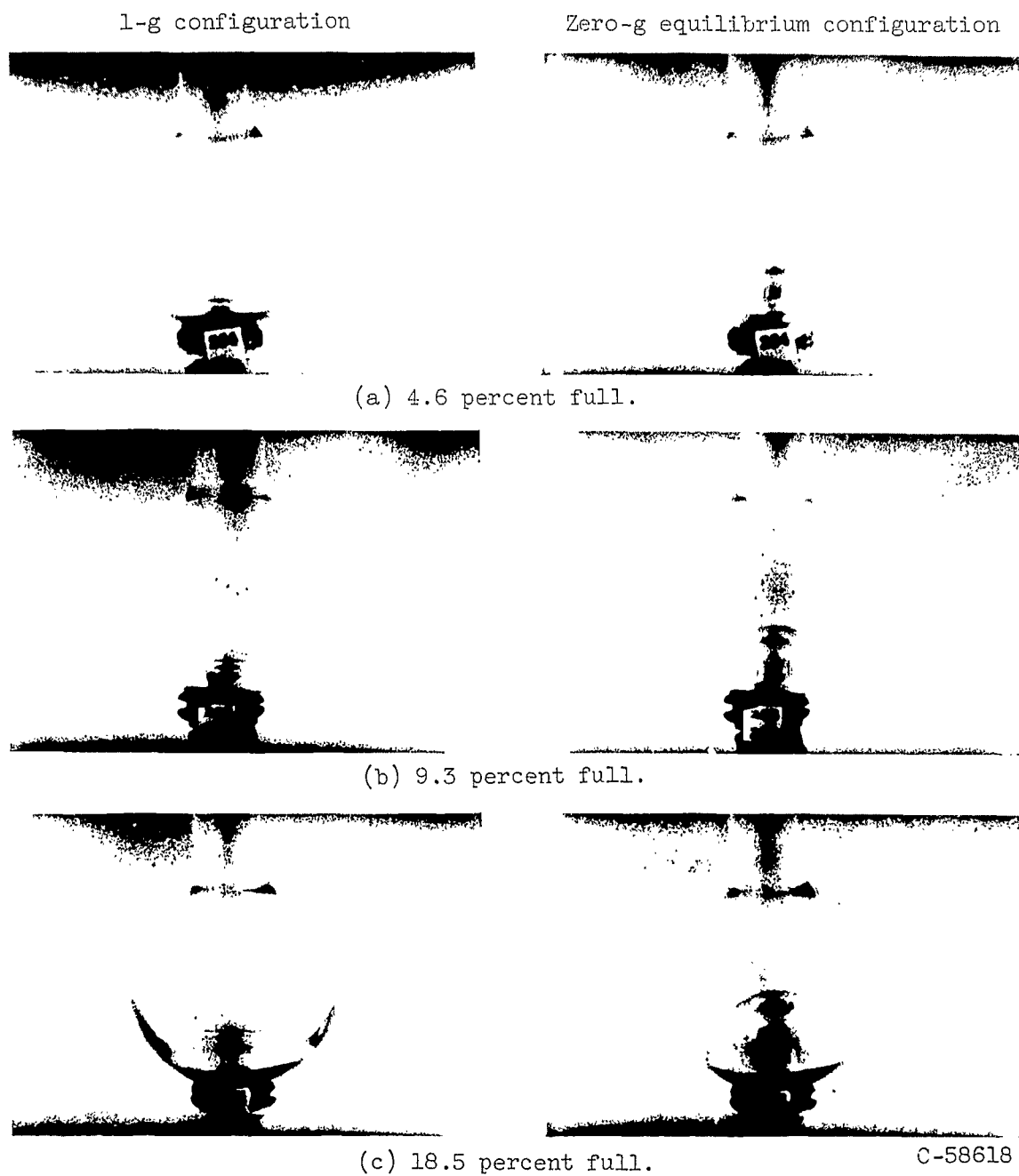
Figure 13. - Mercury in 54-milliliter glass spheres over range of liquid-to tank-volume ratios.

1-g configuration Zero-g equilibrium configuration
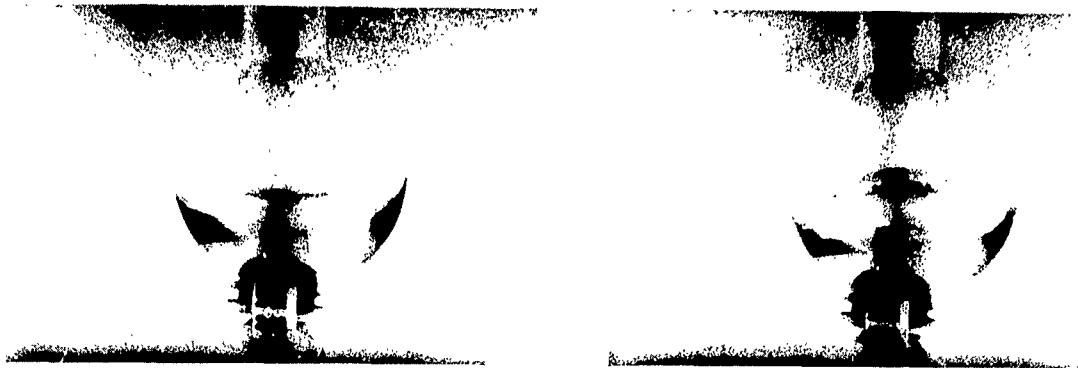
(d) 37.0 percent full.

(e) 55.6 percent full.

(f) 74.1 percent full. C-58619

Figure 13. - Concluded. Mercury in 54-milliliter glass spheres over range of liquid- to tank-volume ratios.

1-g configuration   Zero-g equilibrium configuration

(a) 5 percent full.

(b) 10 percent full.

(c) 20 percent full.   C-58620
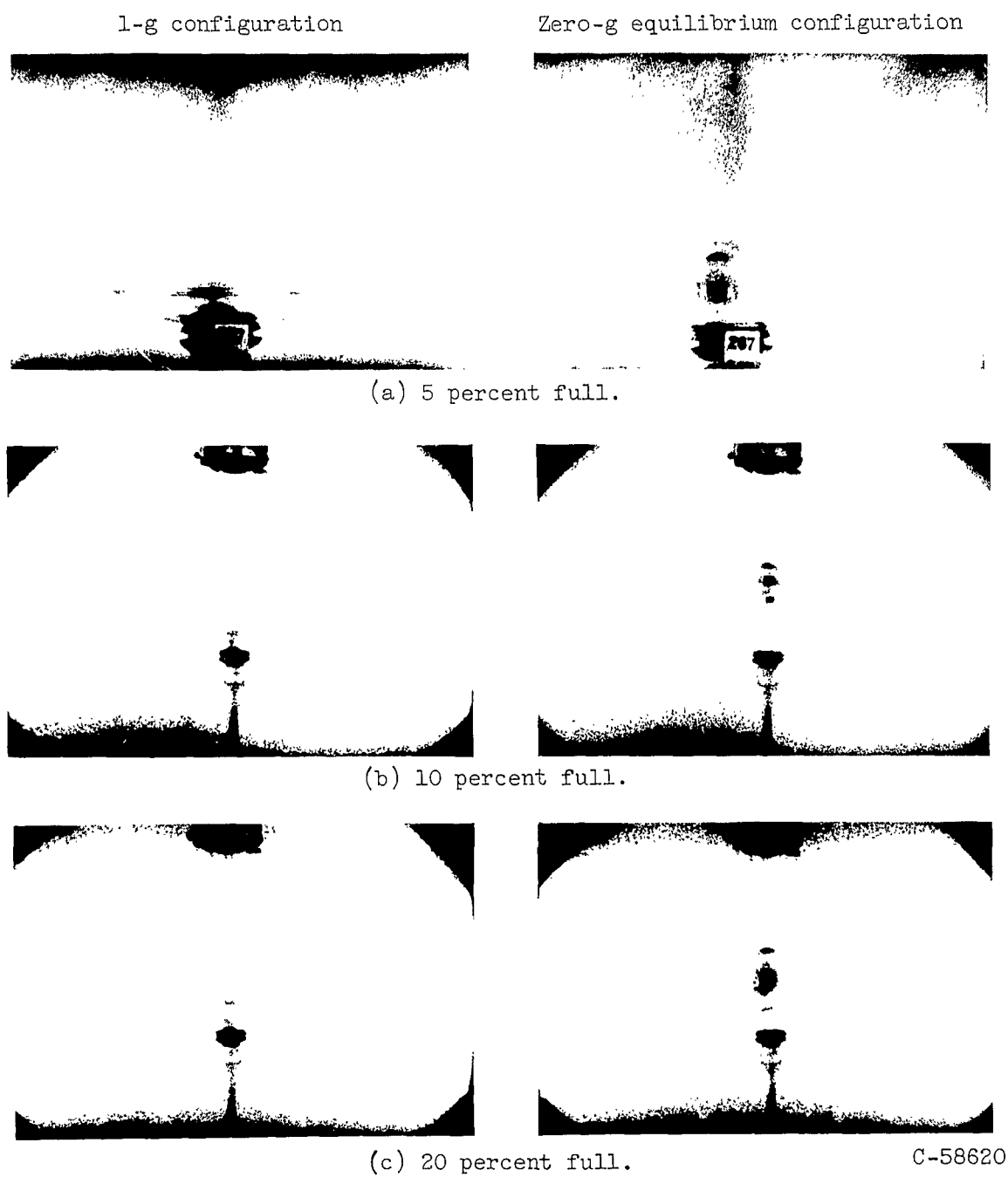
Figure 14. - Mercury in 200-milliliter glass spheres over range of liquid-
to tank-volume ratios.

32

1-g configuration   Zero-g equilibrium configuration
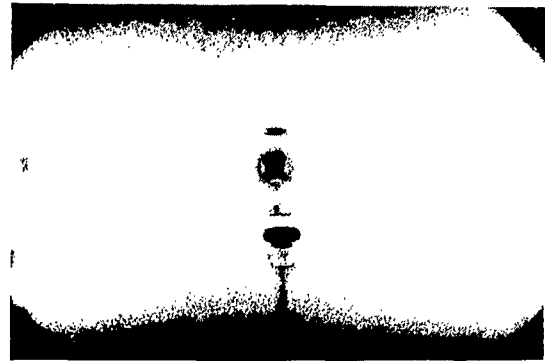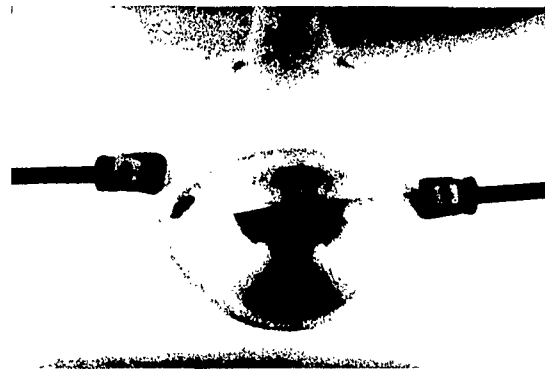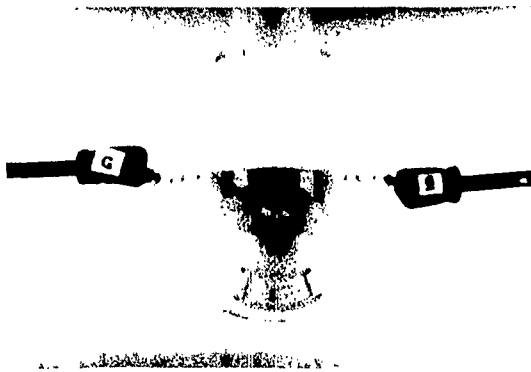
(d) 40 percent full.

(e) 60 percent full.

(f) 80 percent full.   C-58621

Figure 14. - Concluded. Mercury in 200-milliliter glass spheres over range
    of liquid- to tank-volume ratios.

l-g configuration   Zero-g equilibrium configuration

(a) 5 percent full.

(b) 10 percent full.

(c) 20 percent full.   C-58622
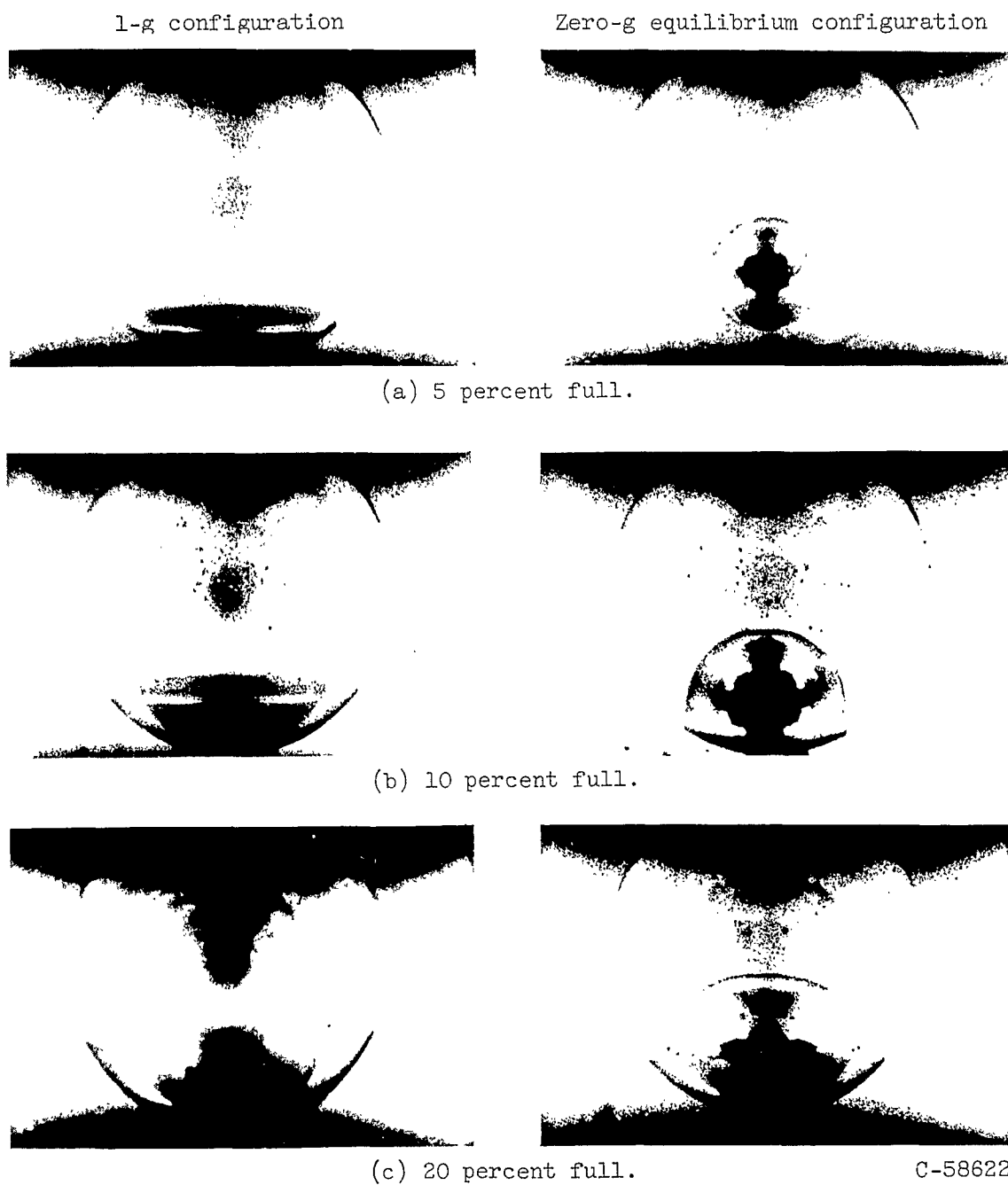
Figure 15. - Mercury in 500-milliliter glass spheres over range of liquid-to tank-volume ratios.

34

1-g configuration   Zero-g equilibrium configuration

(d) 40 percent full.

(e) 60 percent full.

(f) 80 percent full.

Figure 15. - Concluded. Mercury in 500-milliliter glass spheres over range
of liquid- to tank-volume ratios.

1-g configuration   Zero-g equilibrium configuration

(a) 4.7 percent full.

(b) 9.5 percent full.   C-58624
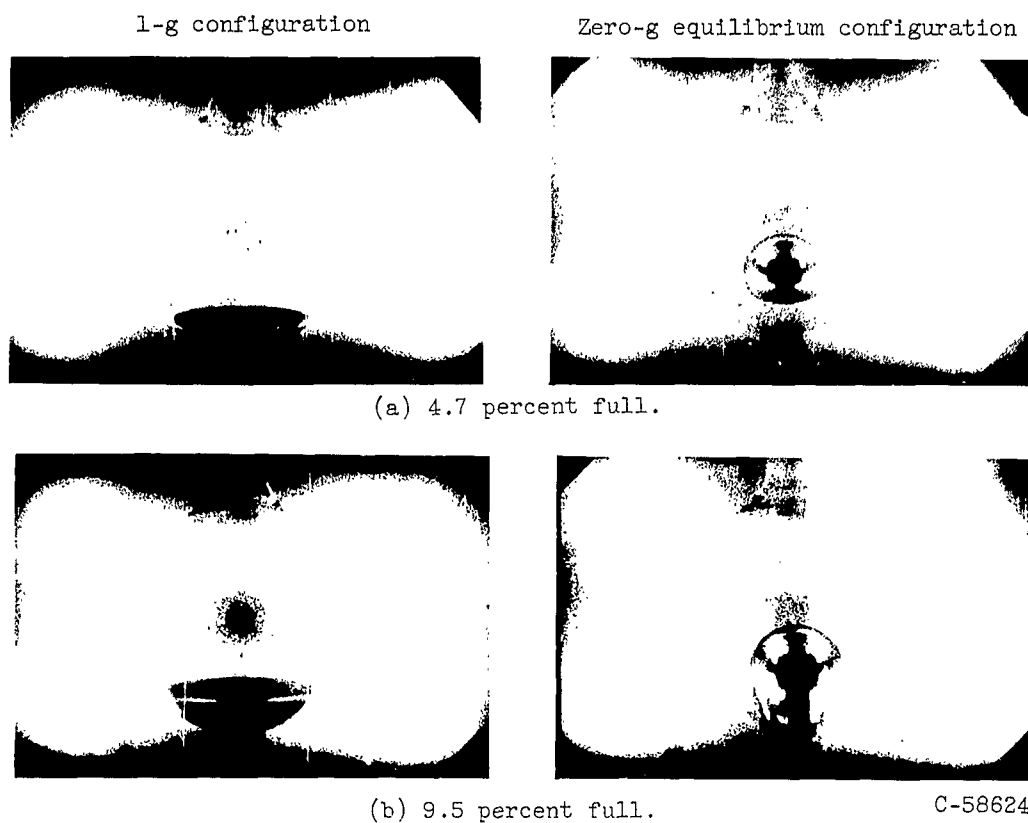
Figure 16. - Mercury in 1068-milliliter glass spheres over range of liquid-to tank-volume ratios.
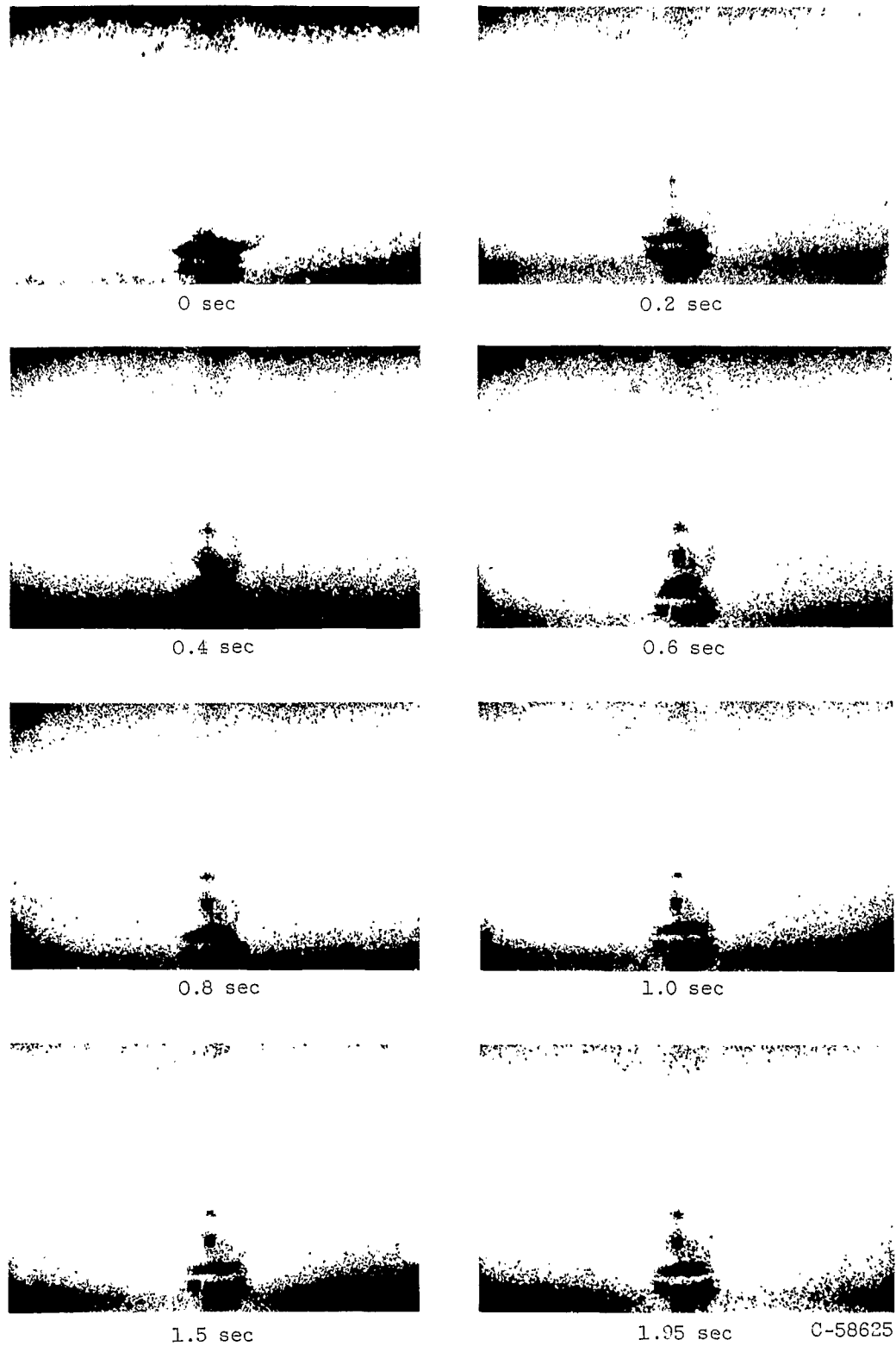
Figure 17. - Mercury in 100-milliliter glass sphere during 1.95 seconds of zero gravity at liquid- to tank-volume ratio of 5 percent.

0 sec   0.2 sec

0.4 sec   0.6 sec

0.8 sec   1.0 sec

1.5 sec   1.05 sec   C-58626
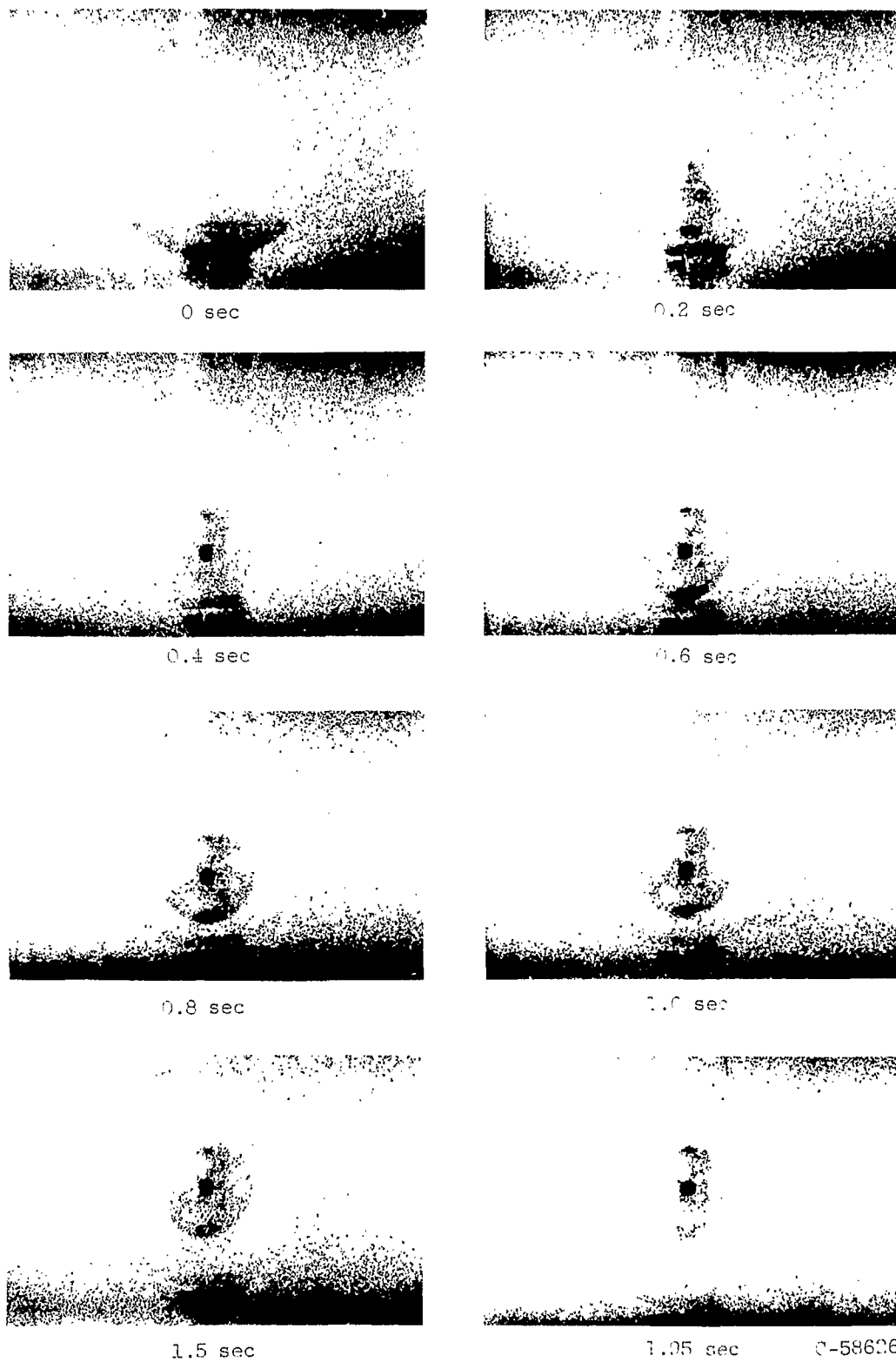
Figure 18. - Mercury in 100-milliliter glass sphere during 1.05 seconds of zero gravity at liquid- to tank-volume ratio of 10 percent.
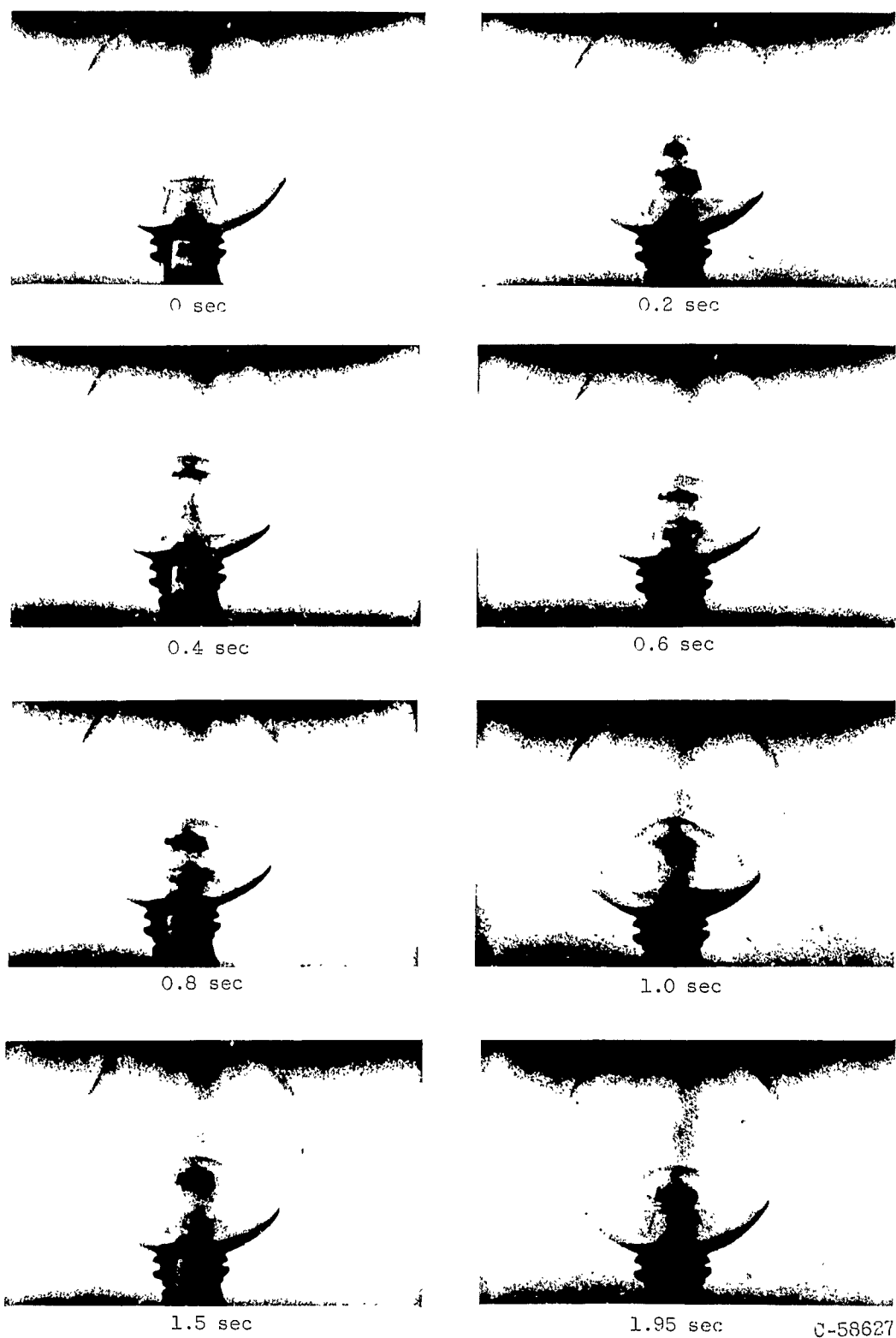
Figure 19. - Mercury in 100-milliliter glass sphere during 1.95 seconds of zero gravity at liquid- to tank volume ratio of 20 percent.
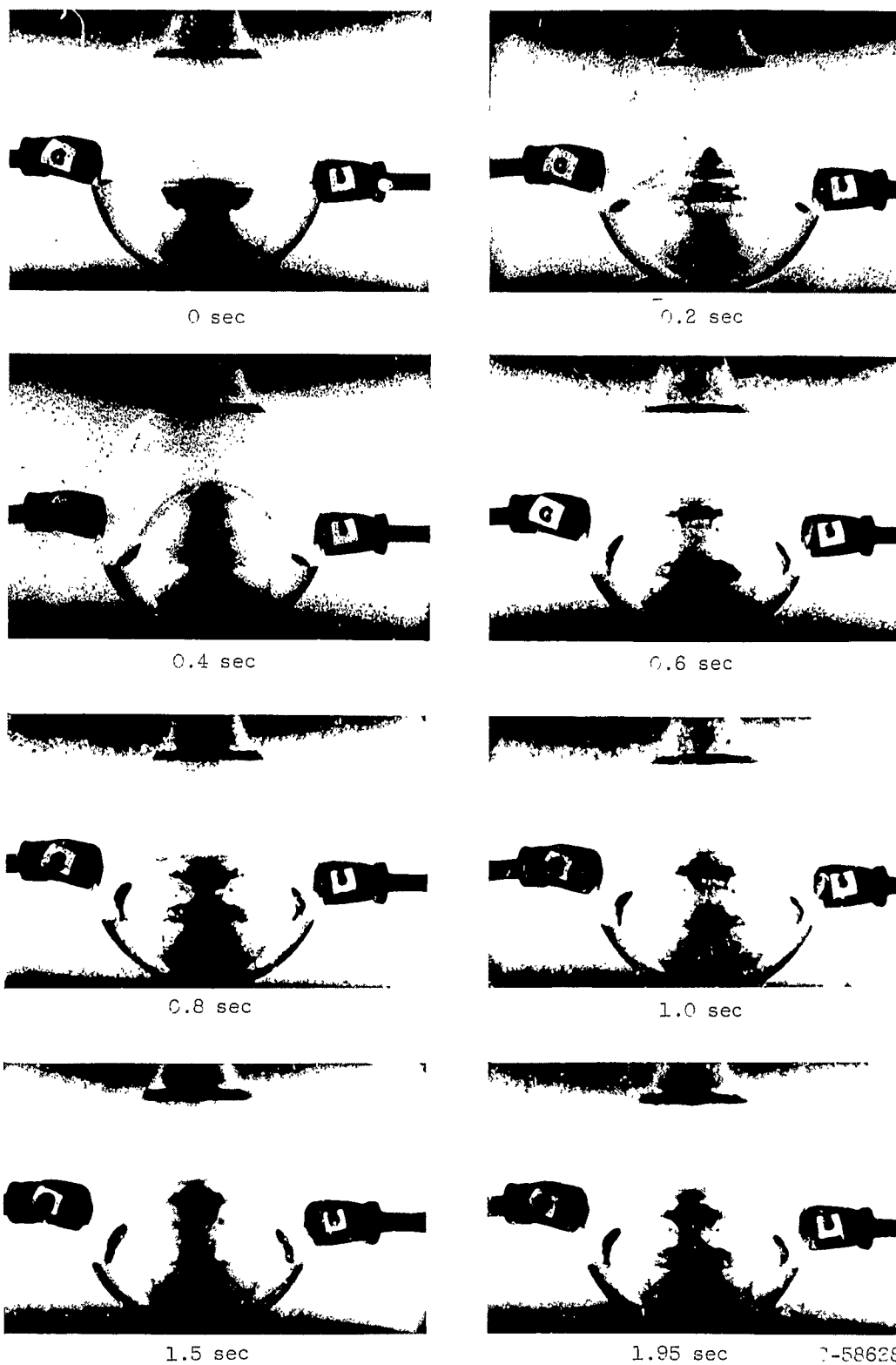
Figure 20. - Mercury in 100-milliliter glass sphere during 1.95 seconds of zero gravity at liquid- to tank-volume ratio of 40 percent.

0 sec

0.2 sec

0.4 sec

0.6 sec

0.8 sec

1. sec

1.5 sec
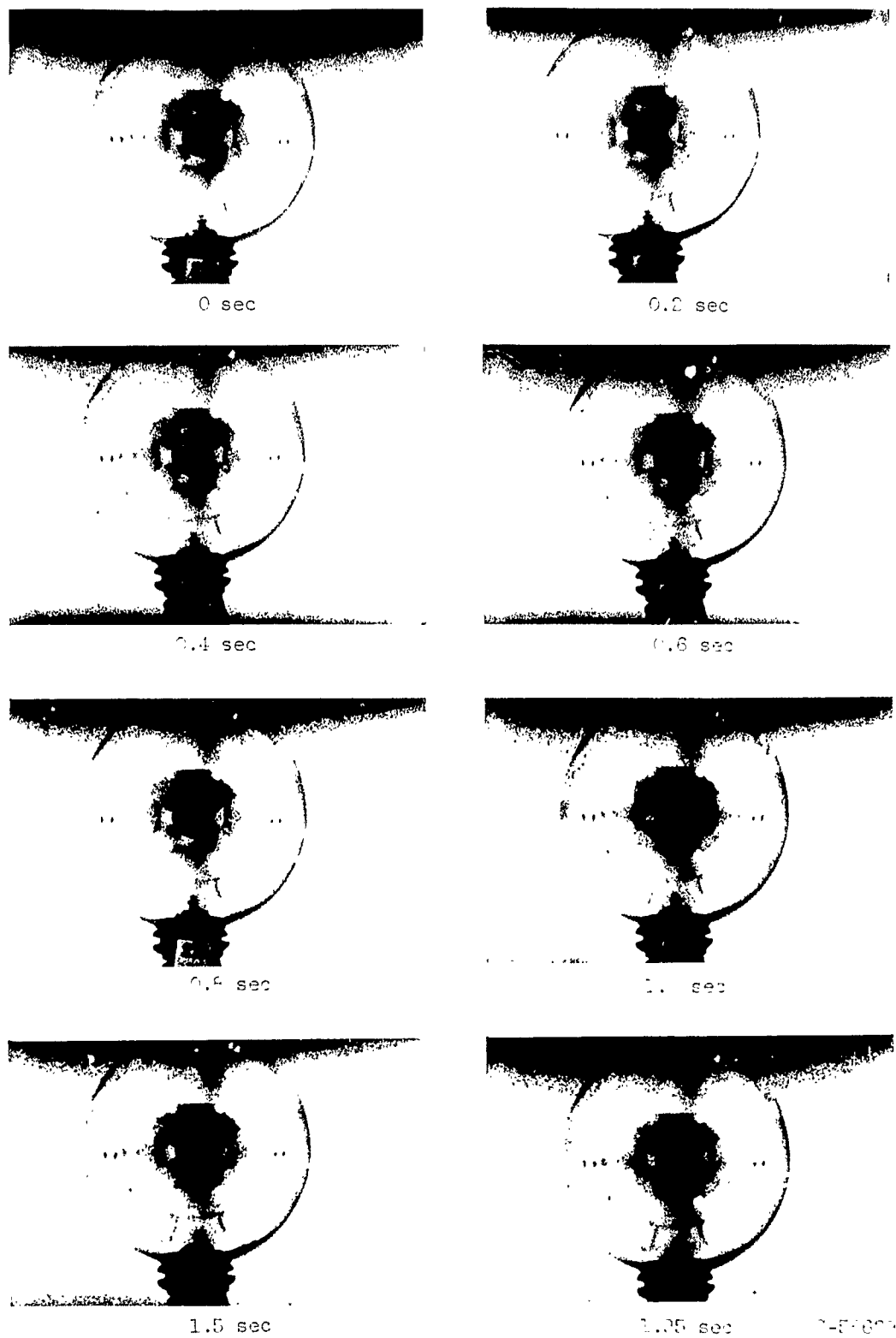
1.95 sec

Figure 21. - Mercury in 1 - milliliter glass sphere during 1.95 seconds of zero gravity at liquid-to-tank-volume ratio of 50 percent.

5B
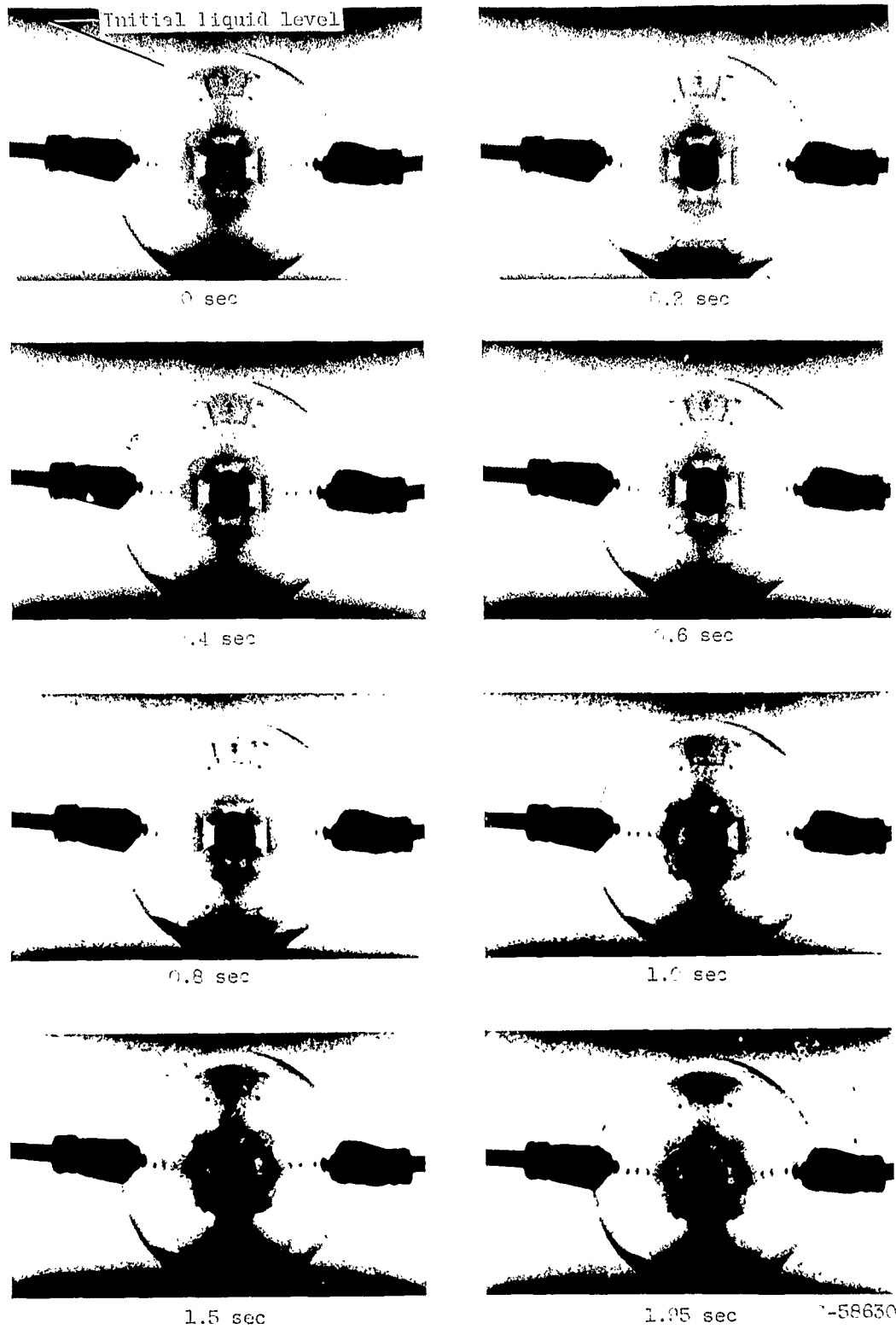
Figure 22. - Mercury in 100-milliliter glass sphere during 1.95 seconds of zero gravity at liquid- to tank-volume ratio of 57 percent.

(a) 30 percent full.

0 sec   1.99 sec

0 sec   1.12 sec   1.26 sec

(b) 40 percent full.

0 sec   0.36 sec   1.65 sec

(c) 46.7 percent full.

0 sec   0.70 sec   .74 sec

(d) 50 percent full.

Figure 3. - Ethyl alcohol in 11-milliliter glass sphere over range of liquid-to-tanker volume ratio.

(e) 74.1 percent full.

0 sec   0.49 sec   0.94 sec

(f) 83.3 percent full.

0 sec   0.41 sec   1.34 sec

(g) 4 percent full.

0 sec   0.31 sec   0.76 sec   -59632
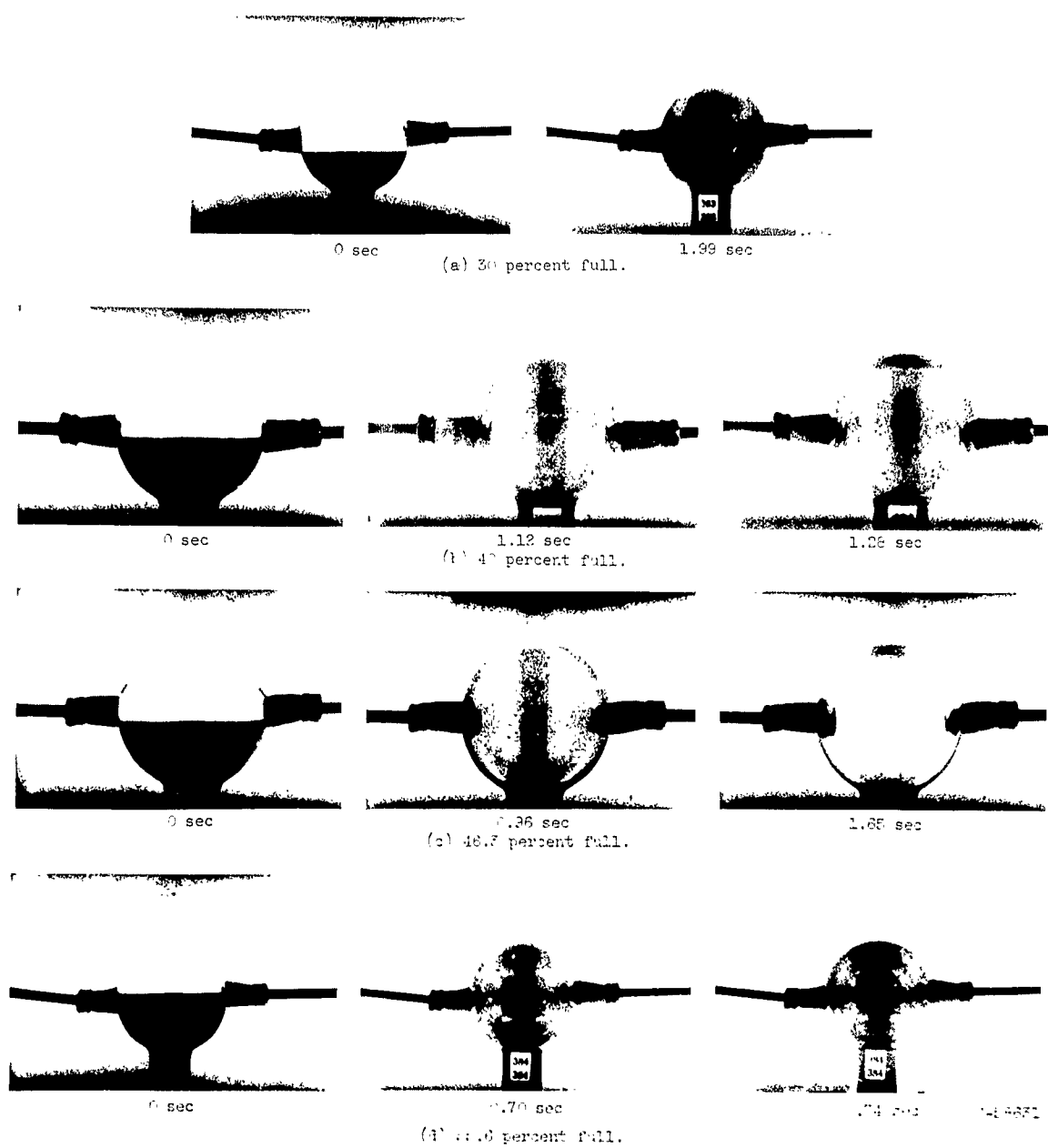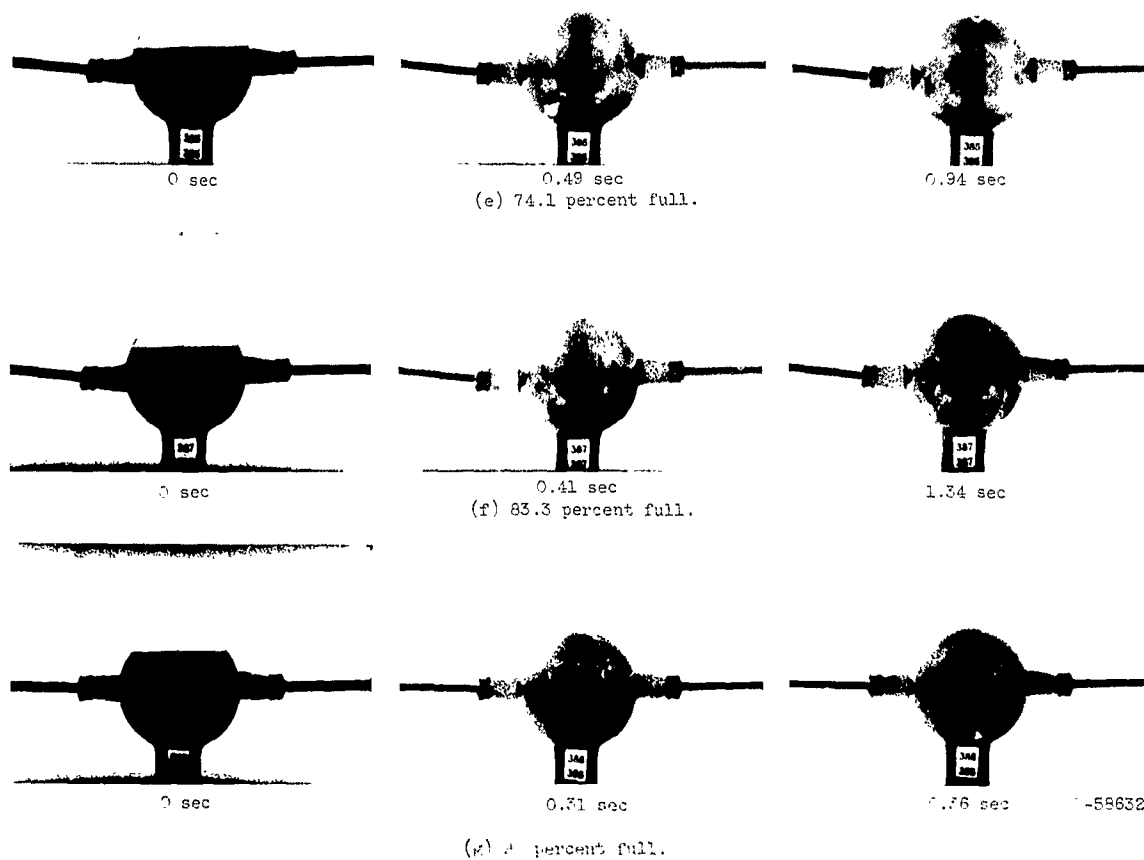
Figure 27. - Concluded. Ethyl alcohol in 64-milliliter glass spheres over range of liquid- to tank-volume ratios.

1.72 sec

(a) 40 percent full.

1.35 sec

1.45 sec

(b) 60 percent full.

1.44 sec

(c) 80 percent full.

(d) 90 percent full.

L-E4673

Figure 31. — 40, 60, 80, and 90 percent filled sphere spinning about mean axis of liquid under zero-gravity conditions.

0 sec   1.03 sec   1.19 sec

(e) 60 percent full.

0 sec   0.92 sec   1.19 sec

(f) 70 percent full.

sec   0.98 sec   1.15 sec

(g) 80 percent full.

sec   .70 sec   1.1 sec   2-59654

(h) 90 percent full.

Figure 24. - Continued. Ethyl alcohol in 2 -millimeter glass sphere over range of liquid- to tank-volume ratios.

0 sec   0.70 sec   1.41 sec

(1) 90 percent full.

0 sec   0.57 sec   1.31 sec

(2) 80 percent full.

0 sec   0.81 sec   1.71 sec   C-59655

(3) 70 percent full.

Figure 21. - Welded, high-speed motion-picture photographs of liquid-to-transverse motion.

(a) 50 percent full.

(b) 60 percent full.

(c) 70 percent full.

(d) 80 percent full.

Figure 26. - Ethyl alcohol in 1 -milliliter glass spheres over range of liquid- to tank-volume ratios.

Figure 26. - High speed photographs of 1.9 milliliter glass spheres over range of liquid-to-tank-volume ratios.

50

(e) 44.3 percent full.

(f) 37.2 percent full.

(g) 45.1 percent full.

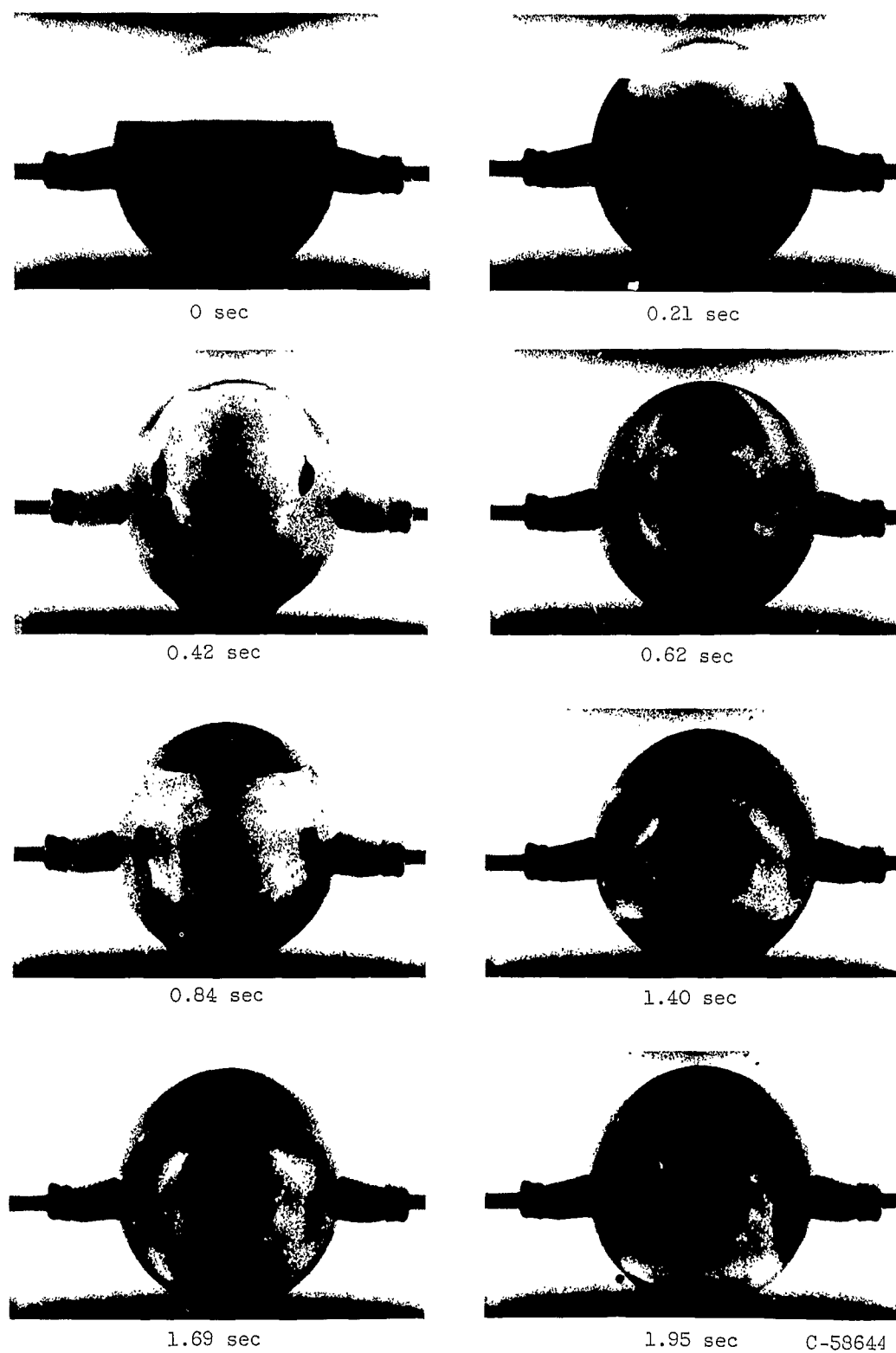Figure 26. - Concluded. Ethyl alcohol in 1 d-milliliter glass sphere over range of liquid- to tank-volume ratios.

Figure 27. - Ethyl alcohol in 100-milliliter glass sphere during 1.75 seconds of zero gravity at liquid- to tank-volume ratio of 35 percent.
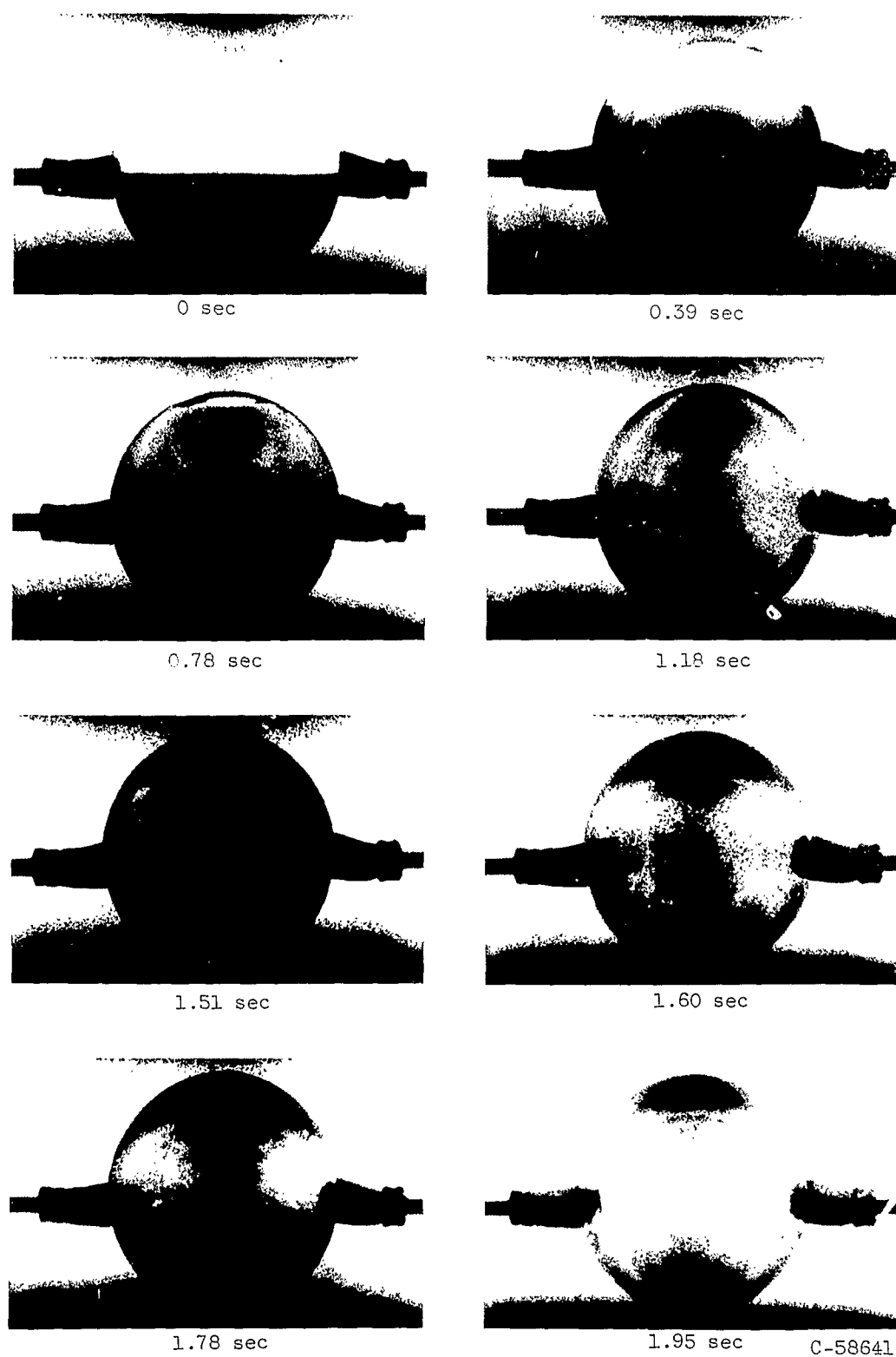
Figure 28. - Ethyl alcohol in 100-milliliter glass sphere during 1.95 seconds of zero gravity at liquid- to tank-volume ratio of 40 percent.
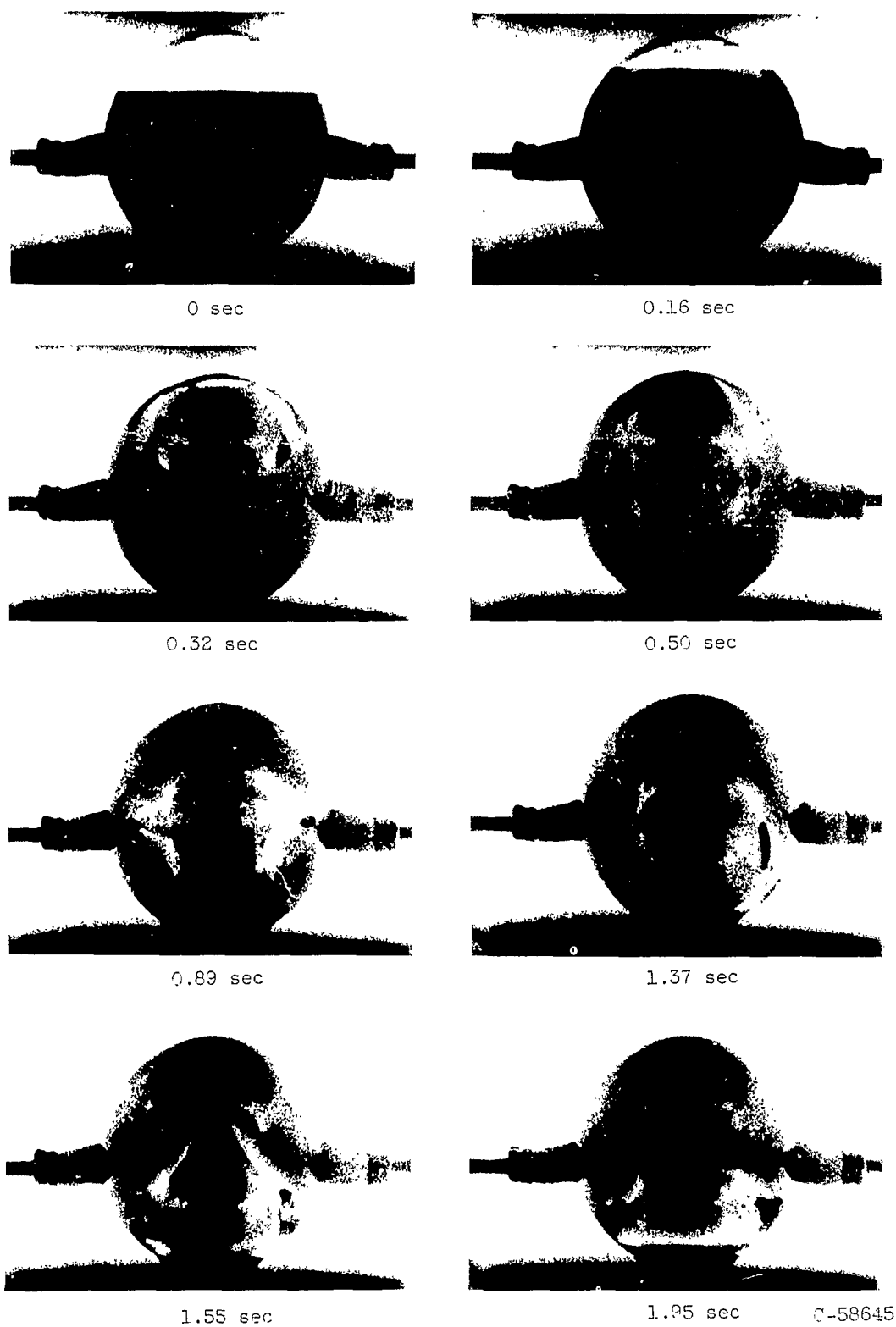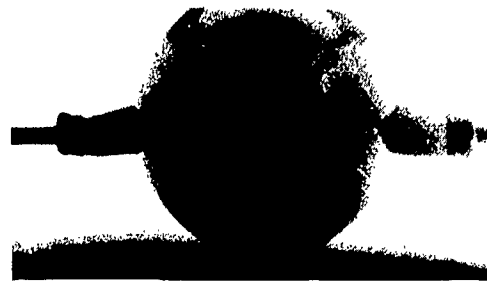
0 sec

0.31 sec

0.62 sec

0.94 sec

1.47 sec

1.65 sec

1.93 sec

1.95 sec   C-58642
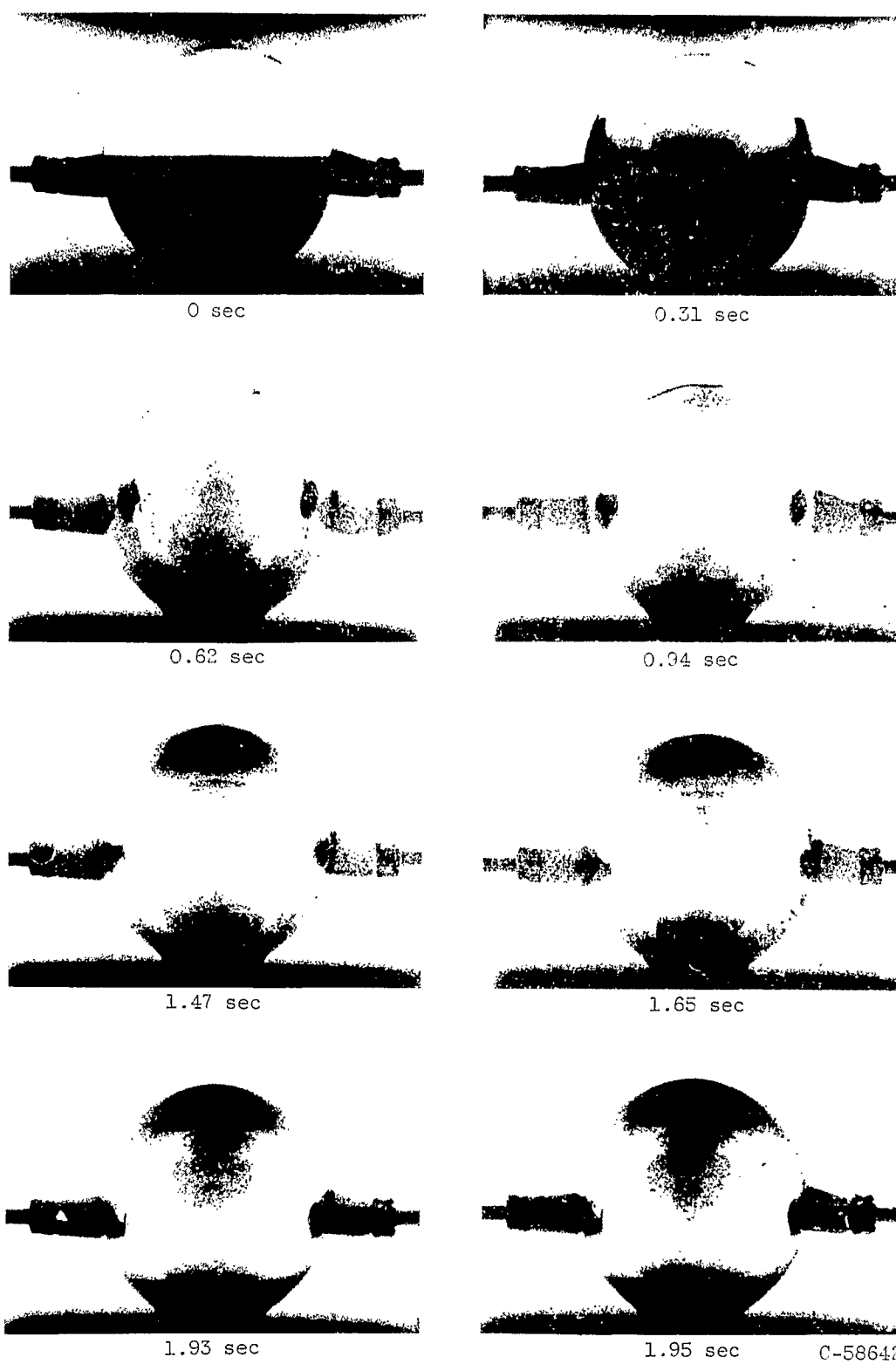
Figure 29. - Ethyl alcohol in 100-milliliter glass sphere during 1.95 seconds
of zero gravity at liquid- to tank-volume ratio of 50 percent.
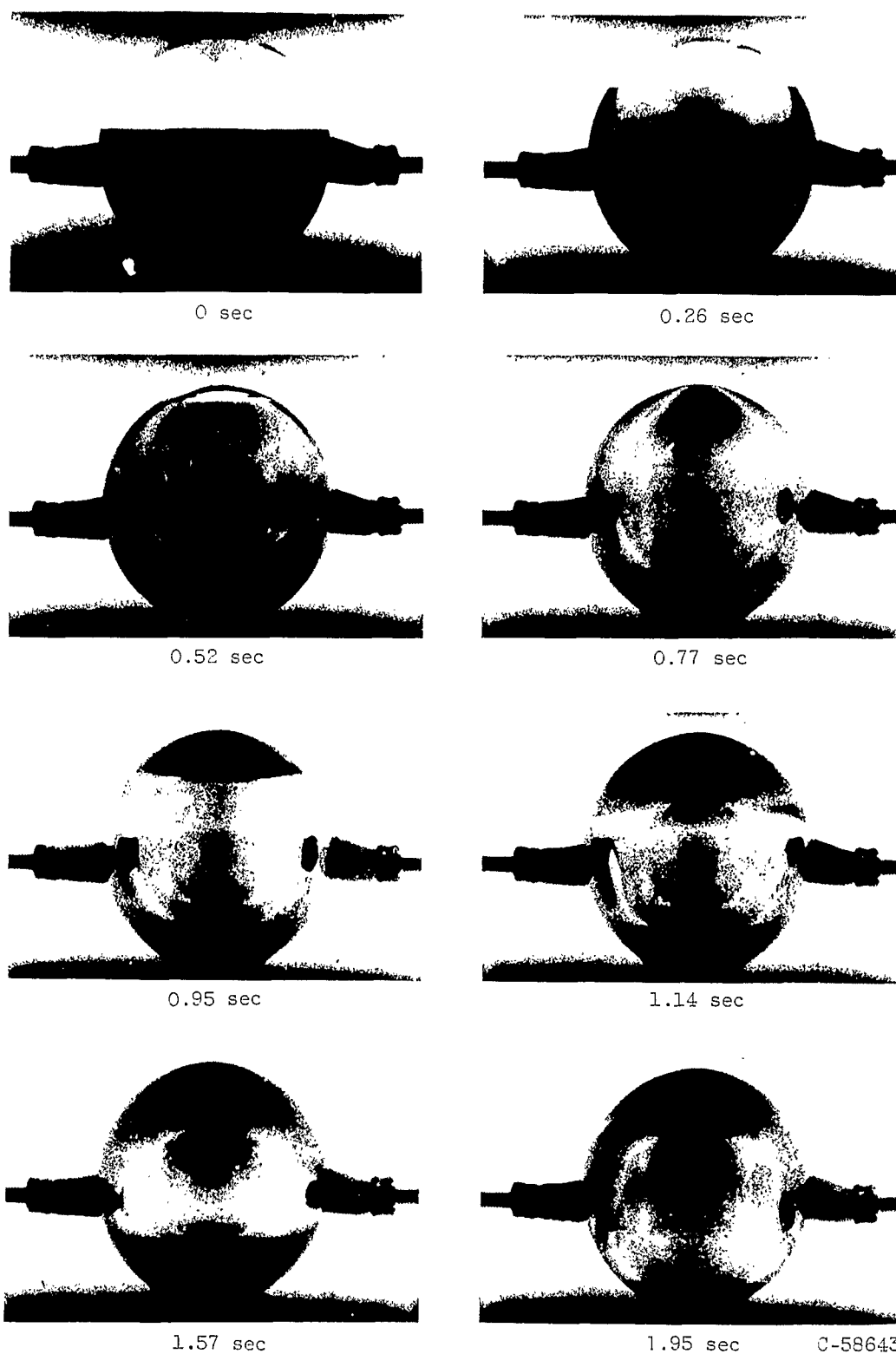
Figure 30. - Ethyl alcohol in 100-milliliter glass sphere during 1.95 seconds of zero gravity at liquid- to tank-volume ratio of 60 percent.

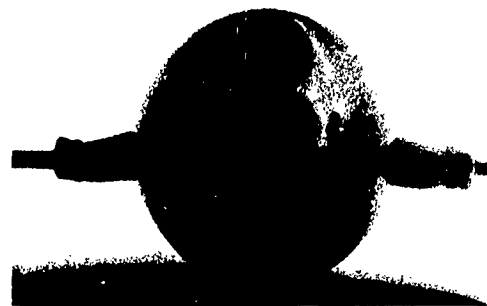Figure 31. - Ethyl alcohol in 100-milliliter glass sphere during 1.95 seconds of zero gravity at liquid- to tank-volume ratio of 70 percent.

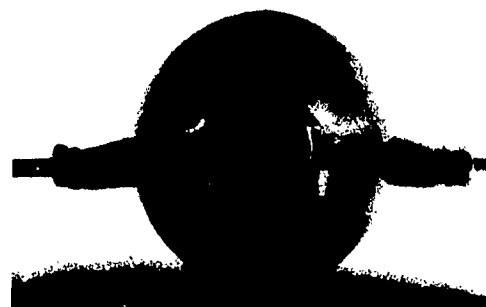Figure 32. - Ethyl alcohol in 100-milliliter glass sphere during 1.95 seconds of zero gravity at liquid- to tank-volume ratio of 80 percent.
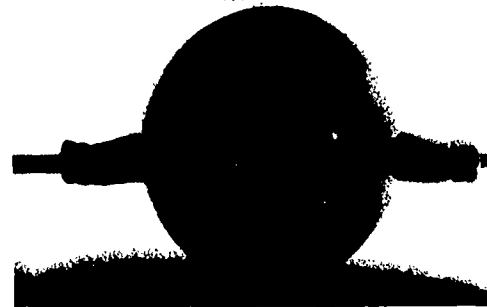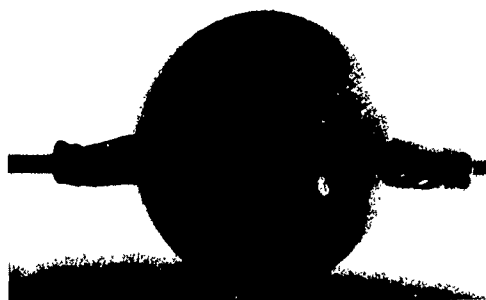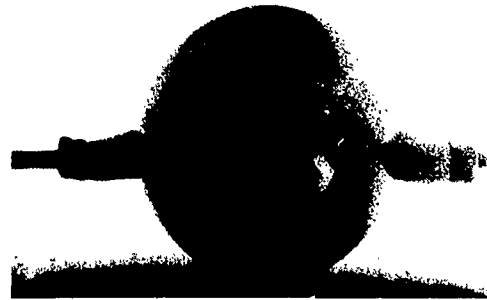
Figure 33. - Ethyl alcohol in 100-milliliter glass sphere during 1.95 seconds of zero gravity at liquid- to tank-volume ratio of 90 percent.
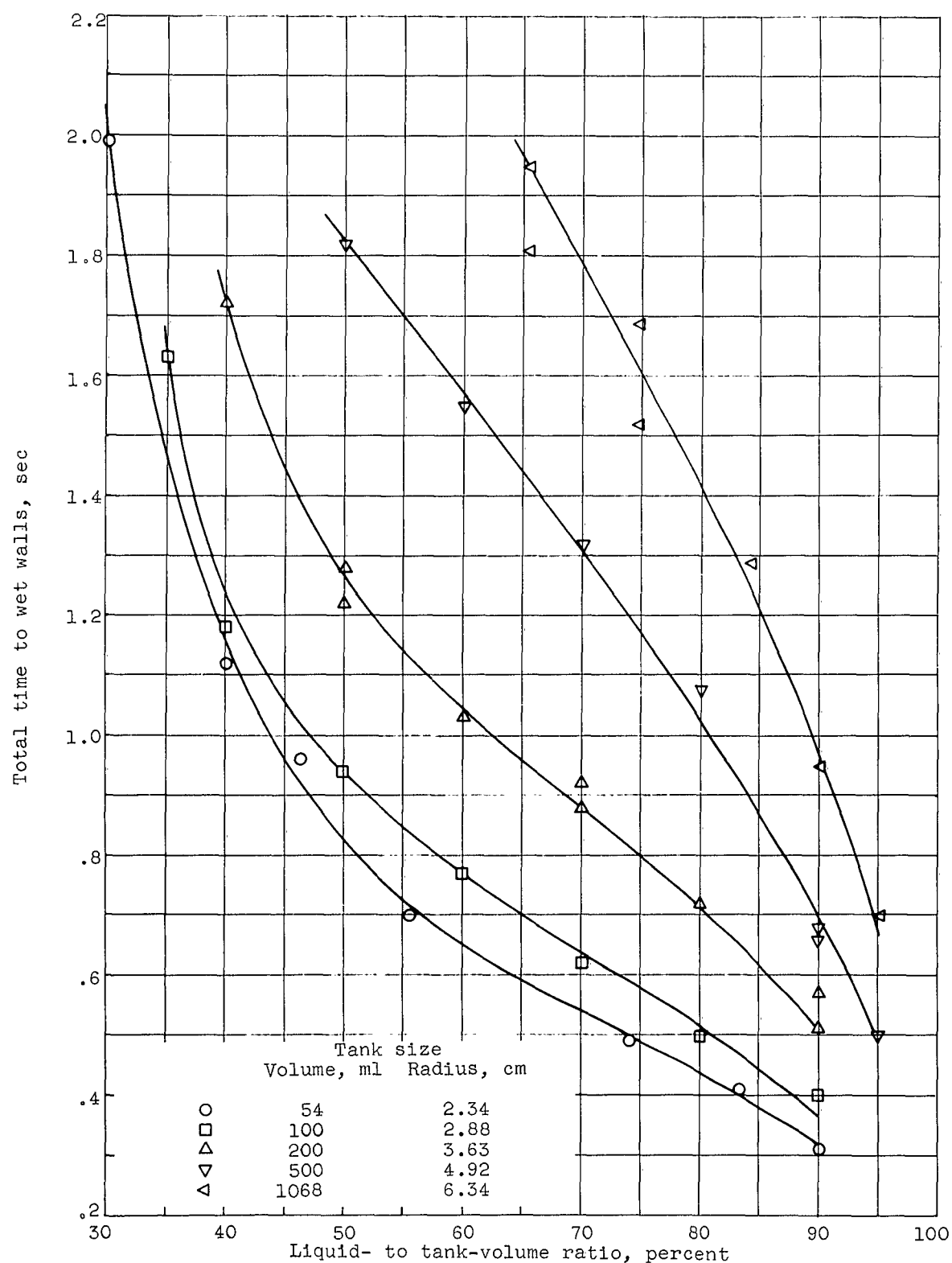
Figure 34. - Total time required for ethyl alcohol to wet tank walls after entering weightlessness as function of volume ratio.
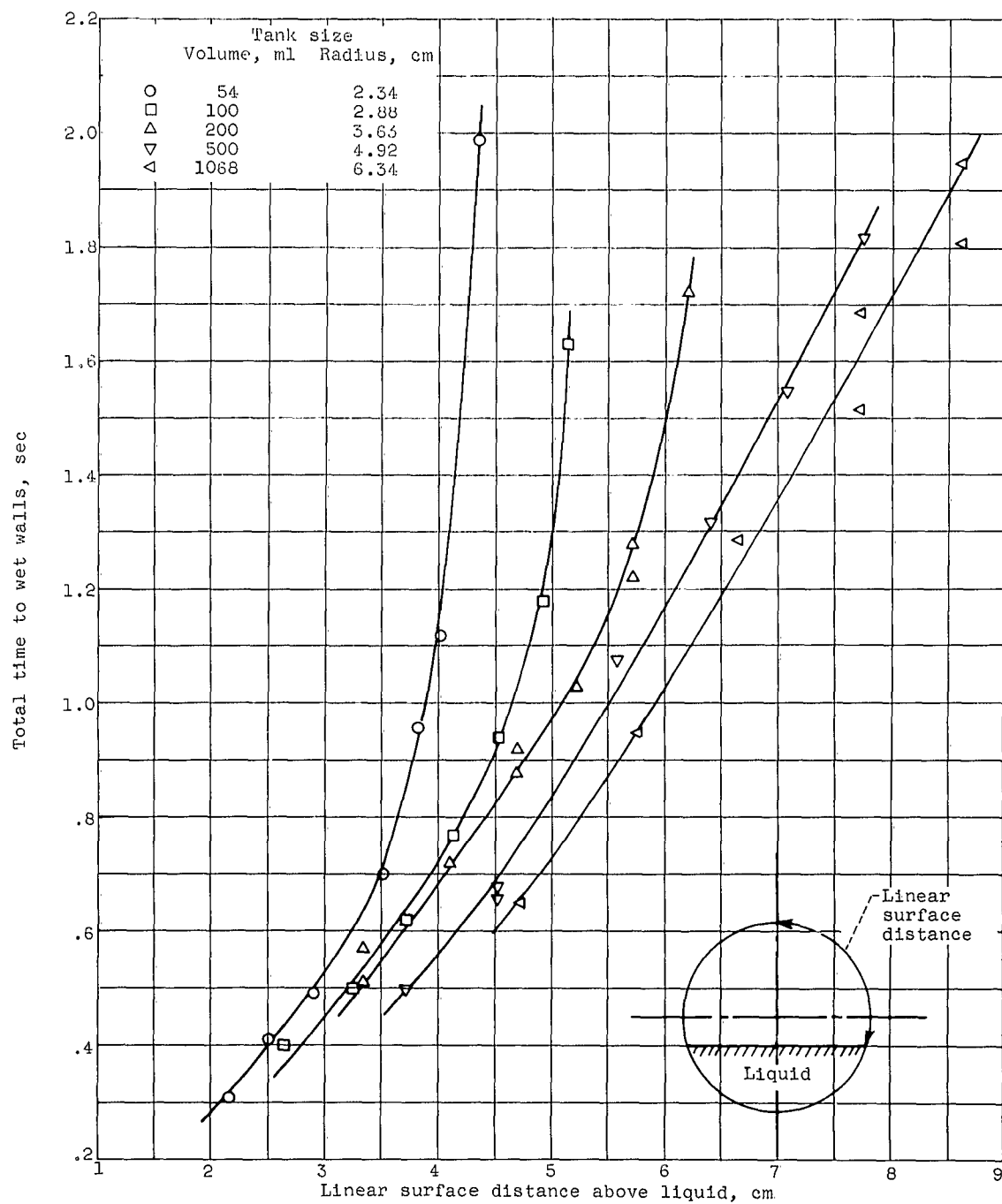
Figure 35. - Total time required for ethyl alcohol to wet tank walls after entering weightlessness as function of distance above liquid.

Figure 36. - Carbon tetrachloride, ethyl alcohol, and water during 1.95 seconds of zero gravity at liquid- to tank-volume ratio of 50 percent.
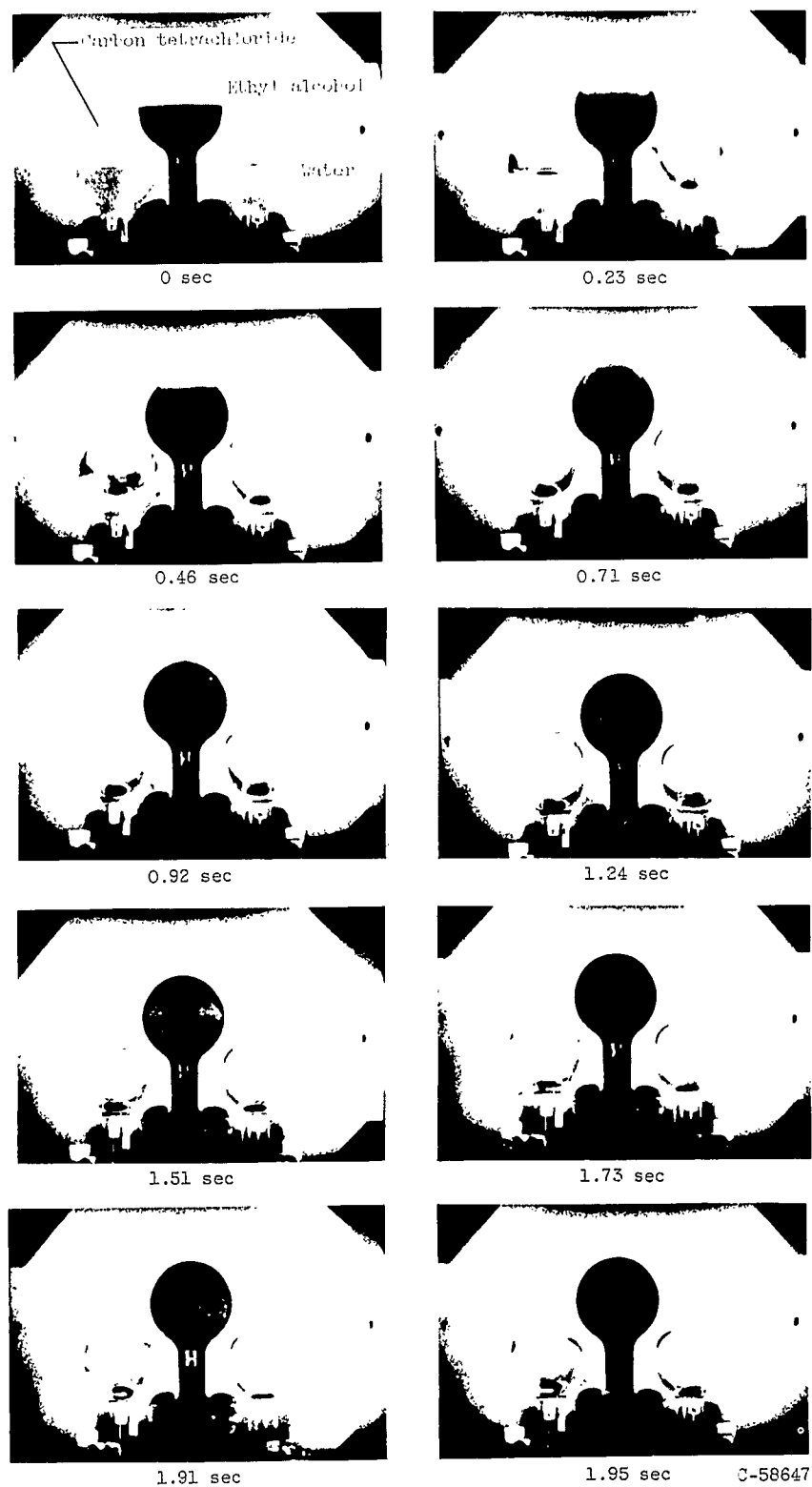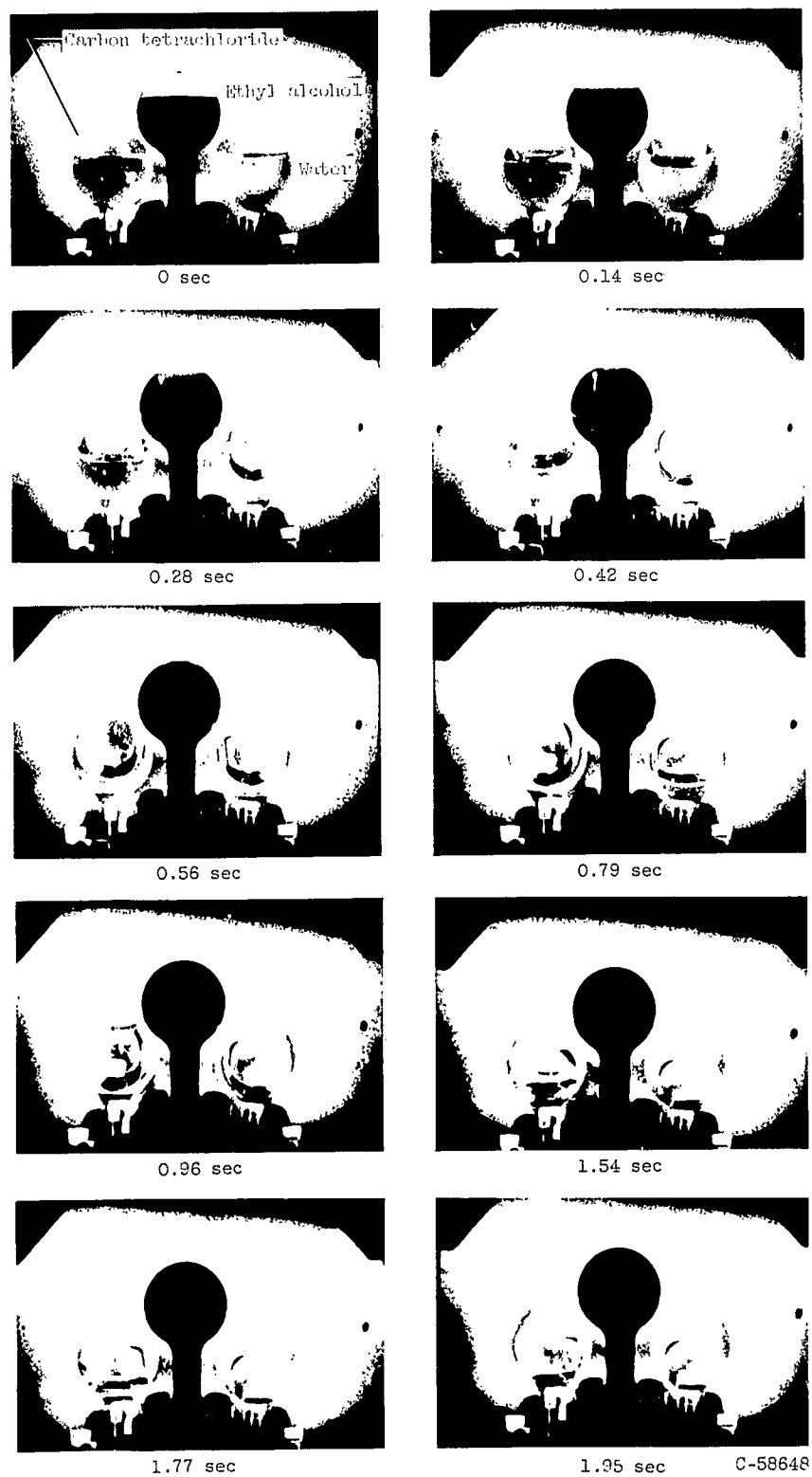
Figure 37. - Carbon tetrachloride, ethyl alcohol, and water during 1.95
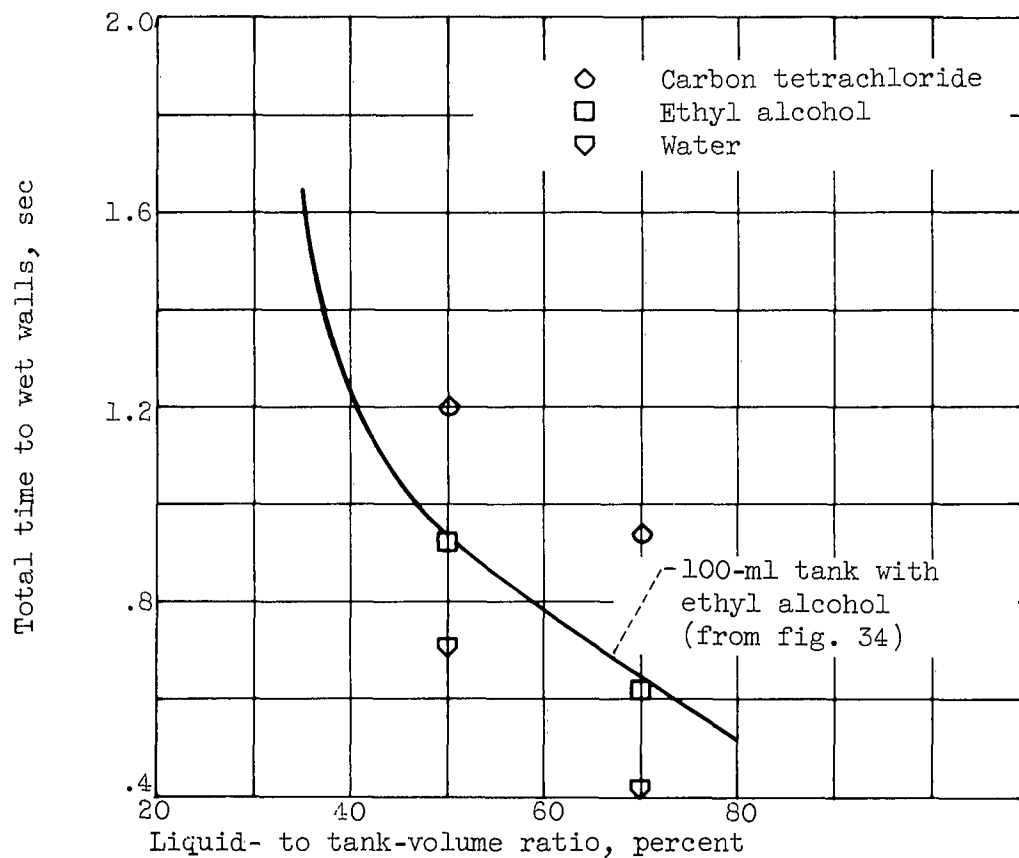seconds of zero gravity at liquid- to tank-volume ratio of 70 percent.

Figure 38. - Comparison of time required to wet tank walls completely for three liquids in 100-milliliter glass spheres.

NASA TN D-1197
National Aeronautics and Space Administration.
EXPERIMENTAL STUDY OF THE EFFECTS OF
WEIGHTLESSNESS ON THE CONFIGURATION OF
MERCURY AND ALCOHOL IN SPHERICAL TANKS.
Donald A. Petrash, Robert F. Zappa, and Edward W.
Otto. April 1962. 62p. OTS price, $1.50.
(NASA TECHNICAL NOTE D-1197)

The behavior of ethyl alcohol and mercury in spherical
glass tanks was experimentally investigated in a zero-
gravity environment. The results indicated that, for
mercury, the equilibrium liquid configuration is such
that the mercury remains in contact with the spherical
tank wall at the same contact angle as was observed
at 1g and the liquid-vapor surface is a surface of
constant curvature. For alcohol, the equilibrium
liquid configuration is a totally wetted tank wall with
a vapor bubble in the interior of the liquid.

Copies obtainable from NASA, Washington

I.   Petrash, Donald A.
II.   Zappa, Robert F.
III. Otto, Edward W.
IV.   NASA TN D-1197

(Initial NASA distribution:
2, Aerodynamics, missiles
and space vehicles;
15, Chemistry, physical;
20, Fluid mechanics;
36, Propellants;
39, Propulsion systems,
liquid-fuel rockets;
45, Research and develop-
ment facilities.)

NASA

NASA TN D-1197
National Aeronautics and Space Administration.
EXPERIMENTAL STUDY OF THE EFFECTS OF
WEIGHTLESSNESS ON THE CONFIGURATION OF
MERCURY AND ALCOHOL IN SPHERICAL TANKS.
Donald A. Petrash, Robert F. Zappa, and Edward W.
Otto. April 1962. 62p. OTS price, $1.50.
(NASA TECHNICAL NOTE D-1197)

The behavior of ethyl alcohol and mercury in spherical
glass tanks was experimentally investigated in a zero-
gravity environment. The results indicated that, for
mercury, the equilibrium liquid configuration is such
that the mercury remains in contact with the spherical
tank wall at the same contact angle as was observed
at 1g and the liquid-vapor surface is a surface of
constant curvature. For alcohol, the equilibrium
liquid configuration is a totally wetted tank wall with
a vapor bubble in the interior of the liquid.

Copies obtainable from NASA, Washington

I.   Petrash, Donald A.
II.   Zappa, Robert F.
III. Otto, Edward W.
IV.   NASA TN D-1197

(Initial NASA distribution:
2, Aerodynamics, missiles
and space vehicles;
15, Chemistry, physical;
20, Fluid mechanics;
36, Propellants;
39, Propulsion systems,
liquid-fuel rockets;
45, Research and develop-
ment facilities.)

NASA

NASA TN D-1197
National Aeronautics and Space Administration.
EXPERIMENTAL STUDY OF THE EFFECTS OF
WEIGHTLESSNESS ON THE CONFIGURATION OF
MERCURY AND ALCOHOL IN SPHERICAL TANKS.
Donald A. Petrash, Robert F. Zappa, and Edward W.
Otto. April 1962. 62p. OTS price, $1.50.
(NASA TECHNICAL NOTE D-1197)

The behavior of ethyl alcohol and mercury in spherical
glass tanks was experimentally investigated in a zero-
gravity environment. The results indicated that, for
mercury, the equilibrium liquid configuration is such
that the mercury remains in contact with the spherical
tank wall at the same contact angle as was observed
at 1g and the liquid-vapor surface is a surface of
constant curvature. For alcohol, the equilibrium
liquid configuration is a totally wetted tank wall with
a vapor bubble in the interior of the liquid.

Copies obtainable from NASA, Washington

I.   Petrash, Donald A.
II.   Zappa, Robert F.
III. Otto, Edward W.
IV.   NASA TN D-1197

(Initial NASA distribution:
2, Aerodynamics, missiles
and space vehicles;
15, Chemistry, physical;
20, Fluid mechanics;
36, Propellants;
39, Propulsion systems,
liquid-fuel rockets;
45, Research and develop-
ment facilities.)

NASA

NASA TN D-1197
National Aeronautics and Space Administration.
EXPERIMENTAL STUDY OF THE EFFECTS OF
WEIGHTLESSNESS ON THE CONFIGURATION OF
MERCURY AND ALCOHOL IN SPHERICAL TANKS.
Donald A. Petrash, Robert F. Zappa, and Edward W.
Otto. April 1962. 62p. OTS price, $1.50.
(NASA TECHNICAL NOTE D-1197)

The behavior of ethyl alcohol and mercury in spherical
glass tanks was experimentally investigated in a zero-
gravity environment. The results indicated that, for
mercury, the equilibrium liquid configuration is such
that the mercury remains in contact with the spherical
tank wall at the same contact angle as was observed
at 1g and the liquid-vapor surface is a surface of
constant curvature. For alcohol, the equilibrium
liquid configuration is a totally wetted tank wall with
a vapor bubble in the interior of the liquid.

Copies obtainable from NASA, Washington

I.   Petrash, Donald A.
II.   Zappa, Robert F.
III. Otto, Edward W.
IV.   NASA TN D-1197

(Initial NASA distribution:
2, Aerodynamics, missiles
and space vehicles;
15, Chemistry, physical;
20, Fluid mechanics;
36, Propellants;
39, Propulsion systems,
liquid-fuel rockets;
45, Research and develop-
ment facilities.)

NASA